European Journal of Control 57 (2021) 1–13

Contents lists available at ScienceDirect

European Journal of Control

journal homepage: www.elsevier.com/locate/ejcon

Discrete-time model-based output regulation of fluid flow systems

Junyao Xie[a], Charles Robert Koch[b], Stevan Dubljevic[a,*]

[a] Department of Chemical and Materials Engineering, University of Alberta, Edmonton, AB T6G 2V4, Canada
[b] Department of Mechanical Engineering, University of Alberta, Edmonton, AB T6G 2V4, Canada

ARTICLE INFO

Article history:
Received 19 February 2020
Revised 11 September 2020
Accepted 22 October 2020
Available online 20 November 2020

Recommended by Prof. T. Parisini

Keywords:
Flow control and manipulation
Distributed parameter systems
Ginzburg–Landau equation
Kuramoto–Sivashinsky equation
Output regulation

ABSTRACT

Model-based discrete-time output regulator design is proposed for fluid flow systems using a geometric approach. More specifically, a class of vortex shedding and falling thin film phenomena modelled by complex Ginzburg–Landau equation (CGLE) and Kuramoto–Sivashinsky equation (KSE) are considered. Differently from a traditional continuous-time controller design, a novel discrete-time modelling technique is proposed in a general infinite-dimensional state-space setting, which does not pertain any spatial approximation or model reduction, and preserves model intrinsic properties (such as stability, controllability and observability). Based on the time discretized plant model (CGLE and KSE systems) by the Cayley–Tustin method, discrete regulator regulation equations are established and facilitated for an output regulator design to achieve fluid flow control and manipulation. To address model instability, a spectrum analysis is utilized in stabilizing continuous-time CGLE and KSE systems, and a link between discrete- and continuous-time closed-loop system stabilizing gains is established. Finally, the proposed methodology is demonstrated through a set of simulation cases, by which the output tracking, disturbance rejection, and model stabilization are achieved for the considered CGLE and KSE systems.

1. Introduction

Flow control and manipulation play an important role in the realm of aerodynamics and hydrodynamics especially when it comes to drag reduction, lift enhancement and turbulence suppression. Generally speaking, there are mainly three approaches to cope with general fluid dynamics problems, namely, theoretical analysis, numerical simulation, and experimental study. Considering that experimental study often requires a prohibitive amount of time and cost, while numerical simulation heavily relies on advanced computational technology, computing capacity and most importantly on the availability of accurate, robust and flexible dynamic models, this manuscript seeks to propose an computationally efficient, implementable and scalable modelling method for fluid flow output regulation and manipulation.

Differently from the dynamics of lumped parameter systems, fluid dynamics often take place in both time and space domains and their states evolve on infinite-dimensional Hilbert spaces, which requires relatively complex spatiotemporal modelling techniques. Mathematically stated, most fluid dynamics models are governed by partial differential equations (PDEs) and/or delay equations, leading to general distributed parameter systems (DPSs). For instance, the complex Ginzburg-Landau equation (CGLE) involves a first-order temporal derivative, and first- and second-order spatial derivatives with complex model coefficients, which dramatically increases the difficulty of accurate modelling and corresponding control designs. In addition, one may need to address multiple spatial variables (e.g. three spatial components in the Navier-Stokes equation) and even higher-order derivatives and nonlinear terms (e.g. fourth-order spatial derivative and nonlinear multiplication term in the Kuramoto–Sivashinsky equation (KSE)). Hence, these considerations stated above provide a strong motivation to seek advanced modelling and control techniques for effective and implementable flow control of fluid dynamics systems.

Among the aforementioned fluid dynamics processes, vortex shedding has attracted increasing attention, due to their wide existence manifested by vortex formation when flows pass submerged obstacles with Reynolds numbers larger than the critical values. More specifically, a schematic diagram illustrating the vortex shedding phenomenon in a 2D flow behind a cylinder is given in Fig. 1, where it clearly shows an unstable vortex shedding and its evolution [1]. Additionally, there is also strong interest in falling thin film phenomena described by the Kuramoto–Sivashinsky equation, which as a representative PDE flow model accounts for a wide range of other complex phenomena, such as unstable flame fronts evolution, phase turbulence in Belousov–Zhabotinsky reaction-diffusion systems and interfacial instabilities

* Corresponding author.
E-mail addresses: junyao3@ualberta.ca (J. Xie), bob.koch@ualberta.ca (C. Robert Koch), Stevan.Dubljevic@ualberta.ca (S. Dubljevic).

https://doi.org/10.1016/j.ejcon.2020.10.005
0947-3580/

Fig. 1. Vortex shedding in the 2D flow behind a cylinder [1].

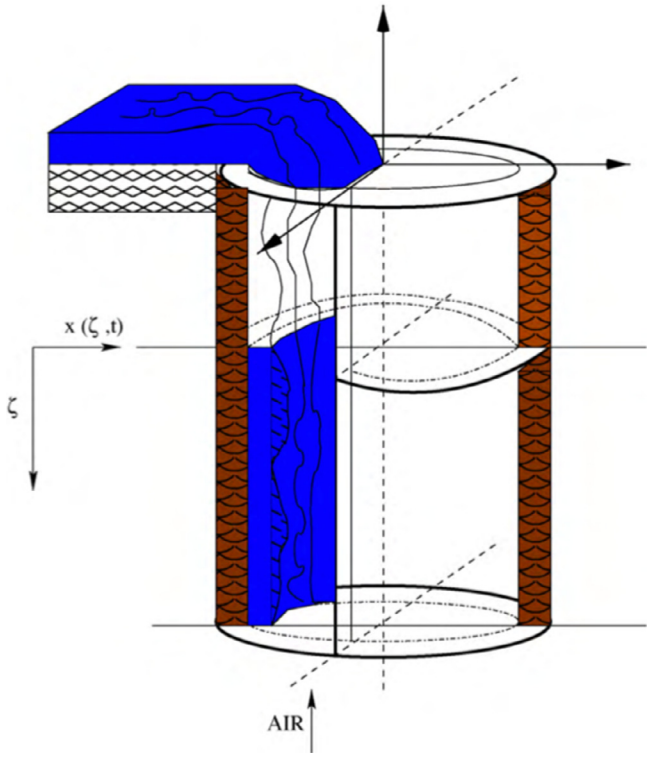

Fig. 2. Schematic framework of a two-phase annular flow in a vertical pipe modelled by Kuramoto–Sivashinsky Equation [18].

between multiple viscous phases [38,43,53]. As shown in Fig. 2, a two-phase annular falling flow in a vertical tube is illustrated using a schematic [18]. For the sake of brevity, this manuscript considers vortex shedding phenomena and falling thin film processes as two representative examples, and review some existing work on modelling and control of CGLE and KSE sequentially.

Regarding vortex shedding analysis and suppression, plenty of studies have been carried out experimentally and using numerical simulation. From an experimental perspective, it has been revealed that the laminar Kármán vortex can be suppressed within a certain range of Reynolds number by several distinct approaches, including: external oscillating the cylinder normal to the mean flow [9], feedback control through suction and blowing treatment on the surface [27,33,51], and acoustic feedback of signals collected from hot-wires in the wake of the cylinder [58]. In addition, the Navier–Stokes equation has been explored to model the dynamics of the cylinder wake theoretically [12,31,47]. However, owing to the inherent complexity of the Navier–Stokes equation, most of the related work has been conducted numerically. On the other hand, the complex Ginzburg–Landau equation with appropriate coefficients was suggested as a simplified model to describe vortex shedding processes in [34]. Along the line of controller designs, a proportional feedback controller was proposed for Kármán vortex shedding suppression with Reynolds numbers close to the critical value ($Re_c \approx 47$ based on the cylinder diameter) [52]. In addition, a non-linear one-dimensional Ginzburg–Landau wake model at 20% above the critical Reynolds number was controlled using a conventional proportional-integral-derivative (PID) controller and a non-linear fuzzy controller [15]. For feedback boundary control, the backstepping approach has been extensively utilized for stabilization of 1D and 2D CGLE systems [1–4]. The developed controllers were validated using computational fluid dynamics (CFD) simulations [44,46] and extended to 3D scenarios [45]. A hybrid method and evolution strategies were deployed to study 2D and 3D vortex evolution of cylinder wakes in [49,50]. From an optimal control perspective, a model predictive controller (MPC) was proposed to solve the problem of CGLE stabilization under consideration of input and state constraints [35]. These studies on CGLE are oriented on stabilizing control while work related to the output regulation of CGLE is limited, which motivates this contribution.

When it comes to flow control of falling thin film processes modelled by the Kuramoto–Sivashinsky equation, many control methods have been developed based on the recent advances in the area of control of distributed parameter systems. Among these, one important contribution lies in the stabilization of the KSE model, including: global stabilization of KSE by in-domain output feedback control [5,14] and through boundary control [37,39]. A single-input-single-output (SISO) and multiple-input-single-output (MISO) boundary model predictive controllers were presented for KSE stabilization in the presence of input and state constraints using a truncated modal decomposition [18,19,60]. A zero dynamics inverse design method was proposed for tracking regulation of a nonlinear KSE with two boundary actuators [11]. For sampled-data control of KSE, a spatially distributed controller was constructed for local stabilization of KSE by using a time-delay approach and a descriptor method [36]. Recently, a delayed boundary controller was designed for global stabilization of a linear KSE by means of the spectral decomposition and the Artstein transform [28]. Although these contributions have provided elegant solutions and controller designs to guarantee the exponential stability of the closed-loop system, most of them are conducted in a continuous-time setting, which at the implementation level needs to be realized in a computationally feasible setting and in addition brings another layer of complexity and questions to be addressed. Therefore, a realizable sampled-data servo-control design is needed for manipulation of various fluid dynamics systems represented by the complex Ginzburg-Landau equation and the Kuramoto–Sivashinsky equation. Moreover, the realization of continuous-in-time designs in the sampled-data setting with finite computational resources has not been fully addressed since temporal and spatial approximations (and/or model reduction) need to be performed for control algorithm realization with the hope that approximate controllers account for the infinite-dimensional nature of underlying distributed parameter models. Hence, the motivation behind this work is not to take the path of continuous designs first, then approximate at the realization level, but to discretize the model in time by application of structure-preserving Cayley–Tustin discretization (linear system properties including stability, controllability and observability are preserved [29,30]) and conduct discrete-in-time regulator design for complex fluid flow systems without any model lumping or spatial approximation. In this way, both regulator design and control law computation can be accomplished in the natural discrete-time (sampled-data) setting of modern microchips.

Therefore, this manuscript is devoted to the development of effective, computationally realizable and scalable servo controllers in the discrete-time setting for fluid flow output regulation of linear CGLE and KSE systems. In particular, the Cayley–Tustin transform is deployed for infinite-dimensional model discretization in the time domain and it does not induce any spectral decomposition or spatial approximation. Then, the internal model principle [21] is revisited and extended to the output regulation of infinite-dimensional

discrete-time systems. By further establishing a finite-dimensional discrete-time exogenous system, discrete-time regulator equations are formulated and utilized for solving a state feedback regulation problem. As for model stabilization, a pole-shifting approach is employed for continuous PDE models and linked to their discrete counterparts. Additionally, an output feedback regulator design is completed by the development of finite-dimensional (exosystem) and infinite-dimensional (fluid flow-plant) observers. Furthermore, we emphasize that proposed design is applicable for a general class of Riesz-spectral distributed parameter systems, and can be extended to DPS models other than CGLE and KSE systems.

The remainder of the paper is organized as follows. Section 2 presents a necessary preliminary, including: general continuous-time PDE model description, and time discretization with the aid of the Cayley–Tustin approach. In Section 3, a finite-dimensional discrete-time exogenous system is provided and a discrete output regulator design framework is given. To demonstrate the feasibility and effectiveness of the proposed method, two representative PDE flow models, i.e. CGLE and KSE systems, are analyzed in detail. The model formulation, spectrum analysis, analytic resolvent determination, and simulation studies for two models are shown in Sections 4 and 5, respectively. Finally, a conclusion is drawn in Section 6.

2. Preliminary

2.1. Notations

In this manuscript, the following notations are used. Suppose that X and V are two Hilbert spaces and $A : X \mapsto V$ is a linear operator. $\mathcal{L}(X, V)$ denotes the set of linear bounded operators from X to V. If $X = V$, we simply write $\mathcal{L}(X)$. The domain, spectrum, resolvent set and resolvent operator of a linear operator A are denoted by: $\mathcal{D}(A)$, $\sigma(A)$, $\rho(A)$, and $\mathcal{R}(s, A) = (sI - A)^{-1}$ with $s \in \rho(A)$, respectively. We denote the space X_1 as the space $\mathcal{D}(A)$ with the norm $\|x\|_1 = \|(\beta I - A)x\|$, and the space X_{-1} as the completion of X with the norm $\|z\|_{-1} = \|(\beta I - A)^{-1}z\|$, where $\forall x \in \mathcal{D}(A)$, $\forall z \in X$, and $\beta \in \rho(A)$. The constructed spaces are related as follows: $X_1 \subset X \subset X_{-1}$, with each inclusion being dense and continuous embedding [55]. The extension of A to X_{-1} is still denoted as A, and C_Λ represents the Λ-extension of C, i.e., $C_\Lambda x = \lim_{\lambda \to +\infty} \lambda C \mathcal{R}(\lambda, A)x$, where the domain of C_Λ consists of those elements $x \in X$ for which the limit exists. Additionally, the inner product is denoted by $\langle \cdot, \cdot \rangle$, and $L^2(0, l)^m$ with a positive integer m denotes a Hilbert space of a m-dimensional vector of the real functions that are square integrable over $[0, l]$ with a spatial length l.

2.2. Model description

As fluid flow dynamics often take place in both temporal and spatial domains, the mathematical models are described by partial differential equations. In general, we consider a continuous-time infinite-dimensional system having the following abstract form:

$$\frac{\partial x}{\partial t}(\xi, t) = Ax(\xi, t) + Bu(t) + Ed(t),\ x(0) = x_0 \tag{1a}$$

$$y_c(t) = C_c x(\xi, t) + D_c u(t) + F_c d(t),\ t \geq 0 \tag{1b}$$

$$y_m(t) = C_m x(\xi, t) + D_m u(t) + F_m d(t) \tag{1c}$$

on a complex Hilbert space $X = L^2((0, l), \mathbb{C})$, i.e. the spatial state $x(\cdot, t) \in X$, where $\xi \in [0, l]$ and $t \in [0, \infty)$ represent spatial and temporal variables. We denote the input $u(t) \in L^2_{loc}([0, \infty), U)$, disturbance $d(t) \in L^2_{loc}([0, \infty), D)$, and the controlled and measured outputs $y_c(t), y_m(t) \in L^2_{loc}([0, \infty), Y)$, where U, D and Y are assumed to be finite-dimensional Hilbert spaces with $\dim U = \dim D = \dim Y = 1$. Additionally, $A : \mathcal{D}(A) \subset X \mapsto X$ is an infinitesimal generator of a C_0-semigroup $\mathbb{T}_A(t)$ on X. For simplicity, we consider bounded control operators $B \in \mathcal{L}(U, X)$, $D_c, D_m \in \mathcal{L}(U, Y)$ bounded disturbance operators $E \in \mathcal{L}(D, X)$, $F_c, F_m \in \mathcal{L}(D, Y)$, and bounded measured output operator $C_m \in \mathcal{L}(X, Y)$. The controlled output operator $C_c \in \mathcal{L}(X_1, Y)$ is considered to be unbounded and assumed to be admissible for $\mathbb{T}_A(t)$. To account for well-posedness, one needs to replace C_c by C_{Lambda} with $C_\Lambda x = \lim_{\lambda \to +\infty} \lambda C_c \mathcal{R}(\lambda, A)x$, where $x \in X$ and $\lambda \in \rho(A)$. Thus this framework leads to a well-posed system [54–56]. For ease of notation, we will use C_c to denote C_Λ in what follows. The transfer functions can be expressed as:

$$\mathcal{G}_c(s) = C_c \mathcal{R}(s, A)B + D_c \tag{2a}$$

$$\mathcal{T}_c(s) = C_c \mathcal{R}(s, A)E + F_c \tag{2b}$$

$$\mathcal{G}_m(s) = C_m \mathcal{R}(s, A)B + D_m \tag{2c}$$

$$\mathcal{T}_m(s) = C_m \mathcal{R}(s, A)E + F_m \tag{2d}$$

with $s \in \rho(A)$ and $\mathcal{R}(s, A) = (sI - A)^{-1}$ is the resolvent operator, and $\mathcal{G}_c(s)$ and $\mathcal{T}_c(s)$ stand for continuous-time transfer functions from $u(t)$ to $y_c(t)$ and from $d(t)$ to $y_c(t)$, respectively. Likewise, $\mathcal{G}_m(s)$ and $\mathcal{T}_m(s)$ are transfer functions from $u(t)$ to $y_m(t)$ and from $d(t)$ to $y_m(t)$.

2.3. Model time-discretization

In order to preserve system properties (such as stability, controllability, and observability) in a discretization process, the Cayley–Tustin time-discretization approach is facilitated to transform a continuous-time model into its discrete analogue [29,30]. For the considered linear infinite-dimensional continuous-time invariant system (1), one deploys the Crank–Nicolson discretization for a given time discretization interval h as follows:

$$\frac{x(\xi, kh) - x(\xi, (k-1)h)}{h} \approx A\frac{x(\xi, kh) + x(\xi, (k-1)h)}{2} + Bu(kh) + Ed(kh) \tag{3a}$$

$$y_c(kh) \approx C_c \frac{x(\xi, kh) + x(\xi, (k-1)h)}{2} + D_c u(kh) + F_c d(kh) \tag{3b}$$

$$y_m(kh) \approx C_m \frac{x(\xi, kh) + x(\xi, (k-1)h)}{2} + D_m u(kh) + F_m d(kh) \tag{3c}$$

with $x(0) = x_0 \in X$, $k \geq 1$. Above time discretization admits an implicit mid-point integration rule and is reversible in time (namely: symmetric) due to the fact that Eq. (3a) stays invariant when one interchanges $x(\xi, kh) \leftrightarrow x(\xi, (k-1)h)$ and $h \leftrightarrow -h$, see details in [29]. Additionally, this time discretization scheme is symplectic in the sense that it preserves Hamiltonian properties of the system [29]. Simple algebraic manipulations lead to the following infinite-dimensional discrete-time state space model:

$$x_k = A_d x_{k-1} + B_d u_k + E_d d_k \tag{4a}$$

$$y_{ck} = C_{cd} x_{k-1} + D_{cd} u_k + \Upsilon_{cd} d_k \tag{4b}$$

$$y_{mk} = C_{md} x_{k-1} + D_{md} u_k + \Upsilon_{md} d_k \tag{4c}$$

with $x_0 \in X$, $k \geq 1$, where x_k, u_k, d_k, y_{ck} and y_{mk} denote the discrete-time state, input, disturbance, controlled output and measured output. It is noted that the discrete input is given by the integration as $\frac{u_k}{\sqrt{h}} = \frac{1}{h}\int_{(k-1)h}^{kh} u(t)dt$ on the interval $t \in [(k-1)h, kh]$, and it has been shown that the Cayley–Tustin discretization is a convergent time discretization scheme for input-output stable system nodes (with $\dim U = \dim D = \dim Y = 1$) in the sense that $\frac{u_k}{\sqrt{h}}$ converges to $u(t)$ as $h \to 0^+$, see [30]. Similar expressions hold for the approximation of d_k, y_{ck} and y_{mk}. The associated discrete-time operators are given by:

$$\begin{bmatrix} A & B & E \\ C_c & D_c & F_c \\ C_m & D_m & F_m \end{bmatrix} \to \begin{bmatrix} A_d & B_d & E_d \\ C_{cd} & D_{cd} & \Upsilon_{cd} \\ C_{md} & D_{md} & \Upsilon_{md} \end{bmatrix} = \begin{bmatrix} -I + 2\delta\mathcal{R}(\delta, A)\sqrt{2\delta} & \mathcal{R}(\delta, A)B\sqrt{2\delta}\mathcal{R}(\delta, A)E \\ \sqrt{2\delta}C_c\mathcal{R}(\delta, A) & \mathcal{G}_c(\delta) & \mathcal{T}_c(\delta) \\ \sqrt{2\delta}C_m\mathcal{R}(\delta, A) & \mathcal{G}_m(\delta) & \mathcal{T}_m(\delta) \end{bmatrix} \tag{5}$$

where $\mathcal{G}_c(\delta)$, $\mathcal{T}_c(\delta)$, $\mathcal{G}_m(\delta)$, and $\mathcal{T}_m(\delta)$ are the transfer functions $\mathcal{G}_c(s)$, $\mathcal{T}_c(s)$, $\mathcal{G}_m(s)$, and $\mathcal{T}_m(s)$ respectively with s evaluated at $\delta = 2/h \in \rho(A)$. Note that there are feedforward operators D_{cd}, Υ_{cd}, D_{cd} and Υ_{md} introduced in the discrete-time setting (4) after performing the Cayley–Tustin discretization, which are not necessarily present in the continuous model setting (1) (i.e. when $D_c = F_c = D_m = F_m = 0$). Furthermore, we denote the discrete-time transfer functions from u_k to y_{ck} and from d_k to y_{ck} by $\mathcal{G}_{cd}(z) = C_{cd}(zI - A_d)^{-1}B_d + D_{cd}$ and $\mathcal{T}_{cd}(z) = C_{cd}(zI - A_d)^{-1}E_d + \Upsilon_{cd}$ respectively, where $z \in \rho(A_d) \setminus \{-1\}$. Similar definitions hold for transfer functions $\mathcal{G}_{md}(z)$ and $\mathcal{T}_{md}(z)$.

Remark 1. The Cayley–Tustin discretization scheme brings an obvious technical advantage that enables one to avoid direct treatment of unbounded operators in the continuous-time setting by instead dealing with bounded operators in the discrete-time setting.

Remark 2. It is shown that the continuous- and discrete-time transfer functions satisfy the following relationship [30]:

$$\mathcal{G}_{cd}(z) = \mathcal{G}_c\left(\frac{z-1}{z+1}\delta\right), \ \mathcal{T}_{cd}(z) = \mathcal{T}_c\left(\frac{z-1}{z+1}\delta\right), \ z \in \rho(A_d)\setminus\{-1\} \tag{6a}$$

$$\mathcal{G}_c(s) = \mathcal{G}_{cd}\left(\frac{\delta+s}{\delta-s}\right), \ \mathcal{T}_c(s) = \mathcal{T}_{cd}\left(\frac{\delta+s}{\delta-s}\right), \ s \in \rho(A)\setminus\{\delta\} \tag{6b}$$

which provides a way for finding $\mathcal{G}_{cd}(z)$ and $\mathcal{T}_{cd}(z)$ from their continuous counterparts, and vice versa. Thus, a stable, continuous-time transfer function is holomorphic and bounded on $\mathbb{C}^+$ if and only if the corresponding discrete-time transfer function is holomorphic and bounded on $\mathbb{D}^+$, see details in [16,48].

Remark 3. For a conservative infinite-dimensional linear system with a scalar inner transfer function and a zero initial state, the discrete-time state trajectory converges to the corresponding continuous-time one in some Hilbert norm sense as the time discretization interval goes to zero [41]. It was also shown that the discrete state converges to the continuous one as time increases for the first-order evolution differential equations (with zero input) in Hilbert space with bounded and unbounded A operators depending on the smoothness of the initial conditions [6,7,22–24], which was further extended to the cases of initial values problems and boundary values problems of second-order evolution differential equations [25,26,42]. Nevertheless, the state approximation induced by the Cayley–Tustin transformation does not hinder its use in the output regulation problem since transfer functions from the input to the output are preserved from the continuous-time model to the discrete-time one, which plays a central role in the context of output regulation.

In order to proceed with the regulator design, the following concepts are introduced.

Definition 1. A C_0-semigroup $\mathbb{T}_A(t)$ on the Hilbert space X is exponentially stable if there exist positive constants M and α such that:

$$\|\mathbb{T}_A(t)\| \leq Me^{-\alpha t}, \ \forall t \in [0, \infty) \tag{7}$$

and it is strongly stable if $\|\mathbb{T}_A(t)x\| \to 0$ as $t \to +\infty$ for all $x \in X$. $\mathbb{T}_A(t)$ is β-exponentially stable if (7) holds for $-\alpha < \beta$, i.e., its stability margin is at least $-\beta$. A_d is power stable if there exist positive constants M and $\gamma < 1$ such that:

$$\|A_d^k\| \leq M\gamma^k, \ \forall k \in \mathbb{N} \tag{8}$$

and A_d is strongly stable if $A_d^k x \to 0$ as $k \to +\infty$ for all $x \in X$ [17].

Definition 2. Assume that A is the infinitesimal generator of the C_0-semigroup $\mathbb{T}_A(t)$ on the Hilbert space X, $B \in \mathcal{L}(U, X)$, $C_m \in \mathcal{L}(X, Y)$, where U and Y are finite-dimensional Hilbert spaces. Let $\Sigma(A, B, C_m)$ denote the state linear system $\dot{z}(t) = Az(t) + Bu(t)$, $y(t) = C_m z(t)$, $t \geq 0$, $z(0) = z_0 \in X$, where generating operators A, B, and C_m are defined as above, and state, input and output spaces are X, U, and Y. If there exist $K \in \mathcal{L}(X, U)$ and $L \in \mathcal{L}(Y, X)$ such that $A + BK$ and $A + LC_m$ generate exponentially stable C_0-semigroups $\mathbb{T}_{BK}(t)$ and $\mathbb{T}_{LC}(t)$, then the system $\Sigma(A, B, C_m)$ is exponentially stabilizable and detectable. If $\mathbb{T}_{BK}(t)$ and $\mathbb{T}_{LC}(t)$ are β-exponentially stable, then the system $\Sigma(A, B, C_m)$ is β-exponentially stabilizable and detectable [17].

3. Output regulation

In this section, an output regulator design method is developed for output regulation of a class of infinite-dimensional systems in a discrete-time setting. In particular, a discrete-time output regulator design is proposed for self-adjoint Riesz-spectral PDE systems, based on the discretized distributed parameter flow plant and discrete exogenous system.

3.1. Exogenous system

To construct the disturbance (to be rejected) and the reference signals (to be tracked), a discrete-time finite-dimensional exogenous system (i.e. exo-system) is introduced as follows:

$$q_k = S_d q_{k-1}, \ q_0 = q^0 \in \mathbb{C}^n, \ k \geq 1 \tag{9a}$$

$$d_k = F_d q_k \tag{9b}$$

$$y_{rk} = Q_d q_k \tag{9c}$$

where q_k, d_k, and y_{rk} represent the exogenous state, disturbance, and reference signals in the discrete-time setting. Moreover, S_d denotes a discrete-time evolution matrix of state q_k and is of $n \times n$ dimension. More specifically, it is assumed that S_d has distinct eigenvalues placed on the boundary of the unit disc, i.e., $\lambda_i^d = \lambda_{Re} + \lambda_{Im} j$ where $i = 1, \ldots, n$, $j^2 = -1$, $\lambda_{Re} \in [0, 1]$, $\lambda_{Im} \in [0, 1]$ and $\lambda_{Re}^2 + \lambda_{Im}^2 \geq 1$. Thus, S_d accounts for step-like and sinusoid-like signals. In order to reconstruct the full state information from the reference single y_{rk}, it is assumed that (S_d, Q_d) is observable. Additionally, we suppose that F_d and Q_d have proper dimensions to generate disturbance and reference signals of interest.

3.2. State feedback regulator design

The main purpose of output regulation is to realize system stabilization, disturbance rejection and reference tracking. Normally, it can be mathematically stated as constructing a discrete-time state feedback regulator of the following form:

$$u_k = K_d x_{k-1} + L_d q_k,\ k \geq 1 \tag{10}$$

where $K_d \in \mathcal{L}(X,U)$, $L_d \in \mathcal{L}(\mathbb{C}^n, U)$, such that the following conditions are ensured:

(1) The discrete-time closed-loop system operator $A_d + B_d K_d$ is strongly stable;
(2) The discrete-time tracking error $e_k = y_{ck} - y_{rk} \to 0$ as $k \to +\infty$ for any given $x_0 \in X$ and $q^0 \in \mathbb{C}^n$.

For this design, all state information of the plant and the exosystem is assumed to be known in (10), which literally interprets the definition of "state feedback regulator". Combining the discrete-time plant and exogenous models, the following theorem states the necessary and sufficient condition for the discrete-time state feedback regulator design:

Theorem 1. *Suppose that (A,B) is exponentially stabilizable and $\sigma(S_d) \subset \rho(A_d)$. The discrete state feedback regulation problem is solvable if and only if there exist mappings $\Pi_d \in \mathcal{L}(\mathbb{C}^n, X)$ and $\Gamma_d \in \mathcal{L}(\mathbb{C}^n, U)$ such that the following discrete Sylvester equations hold:*

$$\Pi_d S_d = A_d \Pi_d + (B_d \Gamma_d + P_d) S_d \tag{11a}$$

$$Q_d S_d = C_{cd} \Pi_d + (D_{cd} \Gamma_d + \Theta_{cd}) S_d \tag{11b}$$

where $P_d = E_d F_d$, $\Theta_{cd} = \Upsilon_{cd} F_d$, and $L_d = \Gamma_d - K_d \Pi_d S_d^{-1}$ are utilized to compute the state feedback control law u_k in Eq. (10). Here, E_d and Υ_{cd} are defined in Eqs. (4),(5).

Proof: First, we prove the sufficiency. Substituting Eq. (10) into the discrete system (4) leads to the closed-loop model as follows:

$$x_k = (A_d + B_d K_d) x_{k-1} + (B_d L_d + P_d) q_k \tag{12}$$

By induction, the discrete-time state solution can be found as:

$$\begin{aligned} x_k &= (A_d + B_d K_d)^k x_0 \\ &\quad + \sum_{m=1}^{k} (A_d + B_d K_d)^{m-1} (B_d L_d + P_d) q_{k+1-m} \end{aligned} \tag{13}$$

By substituting Eqs. (9) and (11) into Eq. (13), one obtains:

$$\begin{aligned} &x_k - (A_d + B_d K_d)^k x_0 \\ &= \sum_{m=1}^{k} (A_d + B_d K_d)^{m-1} [B_d (\Gamma_d - K_d \Pi_d S_d^{-1}) + P_d] q_{k+1-m} \\ &= \sum_{m=1}^{k} (A_d + B_d K_d)^{m-1} [(B_d \Gamma_d + P_d) S_d - B_d K_d \Pi_d)] q_{k-m} \\ &= \sum_{m=1}^{k} (A_d + B_d K_d)^{m-1} [\Pi_d S_d - (A_d + B_d K_d) \Pi_d)] q_{k-m} \\ &= \sum_{m=1}^{k} (A_d + B_d K_d)^{m-1} \Pi_d q_{k+1-m} \\ &\quad - \sum_{m=2}^{k+1} (A_d + B_d K_d)^{m-1} \Pi_d q_{k+1-m} \end{aligned} \tag{14}$$

Then, the last expression further induces:

$$x_k = (A_d + B_d K_d)^k (x_0 - \Pi_d q_0) + \Pi_d q_k \tag{15}$$

Moreover, the discrete tracking error can be expressed as:

$$\begin{aligned} e_k &= y_{ck} - y_{rk} \\ &= C_{cd} x_{k-1} + D_{cd} u_k + \Theta_{cd} q_k - Q_d q_k \\ &= (C_{cd} + D_{cd} K_d) x_{k-1} + (D_{cd} L_d + \Theta_{cd} - Q_d) q_k \\ &= (C_{cd} + D_{cd} K_d)(A_d + B_d K_d)^{k-1} (x_0 - \Pi_d q_0) \\ &\quad + [(C_{cd} + D_{cd} K_d) \Pi_d + (D_{cd} L_d + \Theta_{cd} - Q_d) S_d] q_{k-1} \end{aligned} \tag{16}$$

Under the assumption that (A,B) is exponentially stabilizable, it is shown in [16] that (A_d, B_d) is strongly stabilizable with a proper choice of $\delta \in \rho(A)$. Thus we can find $K_d \in \mathcal{L}(X,U)$ such that $A_d + B_d K_d$ is a strongly stable operator, which indicates $(A_d + B_d K_d)^k x \to 0$ as $k \to +\infty$ for all $x \in X$. Therefore, x_k converges to $\Pi_d q_k$ in Eq. (15) and the discrete tracking error e_k goes to zero as $k \to +\infty$ in Eq. (16), which is ensured by the discrete Sylvester Eqs. (11a), (11b).

Now, we show the proof of the necessity by constructing the following extended closed-loop system:

$$\begin{bmatrix} x_k \\ q_k \end{bmatrix} = \begin{bmatrix} A_d + B_d K_d (B_d L_d + P_d) S_d \\ 0 \qquad\qquad S_d \end{bmatrix} \begin{bmatrix} x_{k-1} \\ q_{k-1} \end{bmatrix} \tag{17}$$

It is straightforward to obtain the solution of Eq. (17) by induction as follows:

$$\begin{bmatrix} x_k \\ q_k \end{bmatrix} = \begin{bmatrix} (A_d + B_d K_d)^k x_0 + \sum_{m=1}^{k} (A_d + B_d K_d)^{m-1} (B_d L_d + P_d) q_{k+1-m} \\ S_d^k q_0 \end{bmatrix} \tag{18}$$

Given that $A_d + B_d K_d$ is strongly stable, $(A_d + B_d K_d)^k x_0 \to 0$ as $k \to +\infty$ and Eq. (18) indicates that $[x_k; q_k] \to [\Pi_d q_k; q_k]$ with $k \to +\infty$ and $\Pi_d \in \mathcal{L}(\mathbb{C}^n, X)$. To determine Π_d, we can construct the dynamical evolution of $w_k = [x_k; q_k] - [\Pi_d q_k; q_k]$ as the following homogeneous difference equation:

$$w_k = \begin{bmatrix} A_d + B_d K_d (B_d L_d + P_d) S_d \\ 0 \qquad\qquad S_d \end{bmatrix} w_{k-1} \tag{19}$$

where the initial condition is defined as $w_0 = [x_0; q_0] - [\Pi_d q_0; q_0]$, $w_0 \in \mathcal{H}_e$ with $\mathcal{H}_e = X \bigoplus \mathbb{C}^n$. The first component in Eq. (19) leads to $(A_d + B_d K_d)\Pi_d + (B_d L_d + P_d) S_d = \Pi_d S_d$ which is identical to discrete-time Sylvester Eq. (11a). Furthermore, the discrete tracking error is described as:

$$\begin{aligned} e_k &= y_{ck} - y_{rk} \\ &= C_{cd} x_{k-1} + D_{cd} u_k + \Theta_{cd} q_k - Q_d q_k \\ &= (C_{cd} + D_{cd} K_d) x_{k-1} + (D_{cd} L_d + \Theta_{cd} - Q_d) q_k \\ &= \begin{bmatrix} C_{cd} + D_{cd} K_d & (D_{cd} L_d + \Theta_{cd} - Q_d) S_d \end{bmatrix} \begin{bmatrix} x_{k-1} \\ q_{k-1} \end{bmatrix} \\ &\to [(C_{cd} + D_{cd} K_d) \Pi_d + (D_{cd} L_d + \Theta_{cd} - Q_d) S_d] q_{k-1} \\ &\quad (\text{as } k \to +\infty) \end{aligned} \tag{20}$$

To realize perfect tracking, one needs to ensure that $(C_{cd} + D_{cd} K_d) \Pi_d + (D_{cd} L_d + \Theta_{cd} - Q_d) S_d = 0$, which can be simplified as Eq. (11b) with $L_d = \Gamma_d - K_d \Pi_d S_d^{-1}$. □

By projecting the eigenvalue pair (λ_i^d, ϕ_i^d) of S_d on the discrete Sylvester Eq. (11), it is straightforward to determine the discrete regulator gains (Γ_d, Π_d) as:

$$\Pi_d \phi_i^d = \lambda_i^d (\lambda_i^d I - A_d)^{-1} (B_d \Gamma_d + P_d) \phi_i^d \tag{21a}$$

$$\Gamma_d \phi_i^d = [\mathcal{G}_{cd}(\lambda_i^d)]^{-1} [Q_d - \mathcal{T}_{cd}(\lambda_i^d) F_d] \phi_i^d \tag{21b}$$

where $\mathcal{G}_{cd}(\lambda_i^d)$ is the discrete transfer function from u_k to y_{ck} with z evaluated at $z = \lambda_i^d$. Similarly, $\mathcal{T}_{cd}(\lambda_i^d)$ is the discrete transfer function from d_k to y_{ck} with z evaluated at $z = \lambda_i^d$.

Remark 4. In this design the assumption that $\lambda_i^d \in \sigma(S_d) \subset \rho(A_d)$ can be ensured by adjusting the time discretization interval h. To ensure the solvability of the discrete Sylvester Eq. (11), we need to further assume that $\mathcal{G}_{cd}(\lambda_i^d) \neq 0$, $\forall \lambda_i^d \in \sigma(S_d)$, such that $\mathcal{G}_{cd}(\lambda_i^d)$ is invertible in Eq. (21).

Remark 5. The 1–1 correspondence between discrete- and continuous-time transfer functions shown in Eq. (6) provides a constructive way in evaluating the discrete transfer functions $(\mathcal{G}_{cd}(\lambda_i^d), \mathcal{T}_{cd}(\lambda_i^d))$ by using their continuous counterparts.

For the control law (10), what remains is to provide a convenient way to solve for the stabilizing controller gain K_d. In order to address this issue, the following theorem is proposed:

Theorem 2. *Suppose that a self-adjoint Riesz-spectral operator A is an infinitesimal generator of the C_0-semigroup $\mathbb{T}_A(t)$ on the Hilbert space X, $B \in \mathcal{L}(\mathbb{C}, X)$. Assume that A has simple eigenvalues and the spectrum $\{\lambda_n, \phi_n\}$ of A can be decomposed into an unstable part $\{\lambda_{n_u}^u, \phi_{n_u}^u\}$ (with $\lambda_{n_u}^u \geq 0$) and a stable part $\{\lambda_{n_s}^s, \phi_{n_s}^s\}$ (with $\lambda_{n_s}^s < 0$). Then the discrete stabilizing controller gain $K_d \in \mathcal{L}(X, \mathbb{C})$ can be obtained as $K_d\phi = -\sum_{n_u=1}^N \beta_{n_u}^d \langle \phi, \phi_{n_u}^u \rangle$, where $\beta_{n_u}^d$ satisfies $|\frac{\delta+\lambda_{n_u}^u - \sqrt{2\delta}\beta_{n_u}^d b_{n_u}}{\delta-\lambda_{n_u}^u}| < 1$, with $b_{n_u} = \langle B, \phi_{n_u}^u \rangle \neq 0$, such that the Cayley–Tustin discretized system $A_d + B_d K_d$ is strongly stable, where $\delta = \frac{2}{h} \in \rho(A)$ and h denotes the discretization time interval.*

Proof: Given that a self-adjoint Riesz-spectral operator A is an infinitesimal generator of the C_0-semigroup $\mathbb{T}_A(t)$ on the Hilbert space X, it is straightforward to show that A has the following decomposition:

$$Ax = \sum_{n=1}^{+\infty} \lambda_n \langle x, \phi_n \rangle \phi_n \tag{22}$$

where λ_n and ϕ_n, with $n \in \mathbb{N}$, are eigenvalues and eigenfunctions of A, see [17].

For $\Sigma(A_d, B_d, C_{md})$ obtained by Cayley–Tustin transform (5) of $\Sigma(A, B, C_m)$, it is straightforward to obtain operator decompositions as follows:

$$\mathcal{R}x = \sum_{n=1}^{+\infty} \frac{1}{\delta - \lambda_n} \langle x, \phi_n \rangle \phi_n \tag{23a}$$

$$A_d x = \sum_{n=1}^{+\infty} \frac{\delta + \lambda_n}{\delta - \lambda_n} \langle x, \phi_n \rangle \phi_n \tag{23b}$$

$$B_d x = \sum_{n=1}^{+\infty} \frac{\sqrt{2\delta}}{\delta - \lambda_n} \langle Bx, \phi_n \rangle \phi_n \tag{23c}$$

$$C_{md} x = \sum_{n=1}^{+\infty} \frac{\sqrt{2\delta}}{\delta - \lambda_n} \langle x, \phi_n \rangle C_m \phi_n \tag{23d}$$

Now, it is apparent that by the Cayley–Tustin transform one can map $\lambda_n \in \mathbb{C}^-$ of the S-plane into the interior section of the unit disc on the Z-plane (except -1), and vice versa.

Suppose that the spectrum $\{\lambda_n, \phi_n\}$ of A can be decomposed into an unstable part $\{\lambda_{n_u}^u, \phi_{n_u}^u\}$ (with $\lambda_{n_u}^u \geq 0$) and a stable part $\{\lambda_{n_s}^s, \phi_{n_s}^s\}$ (with $\lambda_{n_s}^s < 0$). By Eq. (III.6) in the reference [10], a bounded stabilizing controller gain K can be chosen as $K\phi = -\sum_{n_u=1}^N \beta_{n_u} \langle \phi, \phi_{n_u}^u \rangle$ with some positive β_{n_u}, so that the finite set of countable unstable eigenvalues of A can be shifted to the left side of the complex plane as follows:

$$(A + BK)x = \sum_{n_u=1}^{N} \lambda_{n_u}^u \langle x, \phi_{n_u}^u \rangle \phi_{n_u}^u - \beta_{n_u} \langle x, \phi_{n_u}^u \rangle B + \sum_{n_s=N+1}^{+\infty} \lambda_{n_s}^s \langle x, \phi_{n_s}^s \rangle \phi_{n_s}^s \tag{24}$$

where N denotes the number of possibly unstable eigenvalues and hence it is the rank of K. Thus, the original continuous-time system is stabilized, see [17].

Furthermore, one can determine the discrete-time stabilizing operator $K_d\phi = -\sum_{n=1}^N \beta_{n_u}^d \langle \phi, \phi_{n_u}^u \rangle$ with some design parameter $\beta_{n_u}^d$ as:

$$(A_d + B_d K_d)x = \sum_{n_u=1}^{N} \left[\frac{\delta + \lambda_{n_u}^u}{\delta - \lambda_{n_u}^u} \langle x, \phi_{n_u}^u \rangle \phi_{n_u}^u - \frac{\sqrt{2\delta}\beta_{n_u}^d}{\delta - \lambda_{n_u}^u} \langle B\langle x, \phi_{n_u}^u \rangle, \phi_{n_u}^u \rangle \phi_{n_u}^u \right] + \sum_{n_s=N+1}^{+\infty} \frac{\delta + \lambda_{n_s}^s}{\delta - \lambda_{n_s}^s} \langle x, \phi_{n_s}^s \rangle \phi_{n_s}^s \tag{25}$$

as it can be ensured that $\langle B, \phi_{n_u}^u \rangle = b_{n_u} \neq 0$ for $n_u = 1, 2, \ldots, N$, it is straightforward to solve the discrete-time stabilizing gain satisfying $|\frac{\delta+\lambda_{n_u}^u - \sqrt{2\delta}\beta_{n_u}^d b_{n_u}}{\delta-\lambda_{n_u}^u}| < 1$. □

Corollary 1. *Under the assumptions in Theorem 2 and $C_m \in \mathcal{L}(X, \mathbb{C})$, the discrete stabilizing output injection gain $L_{1d} \in \mathcal{L}(\mathbb{C}, X)$ can be obtained as $L_{1d}C_{md}\phi = -\sum_{n_u=1}^N \gamma_{n_u}^d \langle \phi, C_{md}^* \rangle \phi_{n_u}^u$, where $\gamma_{n_u}^d$ satisfies $|\frac{\delta+\lambda_{n_u}^u - \sqrt{2\delta}c_{n_u}\gamma_{n_u}^d}{\delta-\lambda_{n_u}^u}| < 1$, with $c_{n_u} = \langle \phi_{n_u}^u, C_m^* \rangle \neq 0$, such that the discretized system $A_d + L_{1d}C_{md}$ using Cayley-Tustin method is strongly stable, where $\delta = \frac{2}{h} \in \rho(A)$ and h denotes the discretization time interval.*

Proof: It is straightforward to show that this is a dual problem of Theorem 2. Hence, the proof can be completed if one takes $C_{md} = B_d^*$ and $L_{1d} = K_d^*$.□

Remark 6. In general, Theorem 2 and Corollary 1 can be extended to the case with A being a general Riesz-spectral operator by finding corresponding eigenfunctions of A^* operator and the case with $U = \mathbb{C}^p$ and $Y = \mathbb{C}^q$ through complex manipulation.

Based on the series expressions in Eq. (23a) and spectral decomposition, one can design a stabilizing controller (and/or observer) gain. For the resolvent and the corresponding discrete operators (A_d, B_d, C_{md}) given by closed-form expressions, we provide the following theorem to guarantee the equivalence of the stability property of the discretized stabilized system using continuous- and discrete-time stabilizing gains by following [16].

Theorem 3. *Given an infinitesimal generator A of the C_0-semigroup $\mathbb{T}_A(t)$ on the Hilbert space X, $B \in \mathcal{L}(\mathbb{C}, X)$, $K \in \mathcal{L}(X, \mathbb{C})$ ensuring that $A + BK$ is exponentially stable, the continuous- and discrete-time stabilizing controller gains are linked by the following expression:*

$$K_d = \sqrt{2\delta}K(\delta - A - BK)^{-1} \tag{26}$$

where $\delta \in \rho(A) \cap \rho(A + BK)$, and $K_d \in \mathcal{L}(X, \mathbb{C})$ is the discrete-time stabilizing gain in the sense that $A_d + B_d K_d$ is strongly stable, where A_d and B_d are the corresponding discrete-time operators of A and B using the Cayley–Tustin transformation.

Proof: The stability of the closed-loop system in the continuous-time $(A_c = A + BK)$ and discrete-time settings $(A_d + B_d K_d)$ are related as follows:

$$\begin{aligned} A_{cd} &= -I + 2\delta(\delta - A_c)^{-1} \\ &= -I + 2\delta(\delta - A - BK)^{-1} \end{aligned} \tag{27}$$

$$A_{dc} = A_d + B_d K_d$$
$$= -I + 2\delta(\delta - A)^{-1} \cdot \left(I + \frac{1}{\sqrt{2\delta}} B K_d\right) \tag{28}$$

where A_{cd} represents the closed-loop system that is first stabilized in the continuous setting by designing a continuous-time stabilizing gain K and then subsequently discretized, while A_{dc} denotes the system that is first discretized in time and then stabilized in the discrete setting by finding a discrete-time stabilizing gain K_d. Hence, by holding the equality of A_{cd} and A_{dc} expressions, one can directly calculate the solution of K_d in terms of K as follow:

$$K_d = \sqrt{2\delta} K (\delta - A - BK)^{-1} \tag{29}$$

Hence the proof is completed and it demonstrates the invariance of the Cayley–Tustin discretization with respect to closed-loop stabilization. □

Corollary 2. *For an infinitesimal generator A of the C_0-semigroup $\mathbb{T}_A(t)$ on the Hilbert space X, $C_m \in \mathcal{L}(X, \mathbb{C})$, the continuous- and discrete-time stabilizing output injection gains can be linked by $L_{1d} = \sqrt{2\delta}(\delta - A - LC_m)^{-1} L$, such that the discretized observer error systems $A_{do} = A_d + L_{1d} C_{md}$ and $A_{od} = -I + 2\delta(\delta - A - LC_m)^{-1}$ share the same stability property by using continuous- and discrete-time output injection gains $L \in \mathcal{L}(\mathbb{C}, X)$ and $L_{1d} \in \mathcal{L}(\mathbb{C}, X)$ based on the Cayley–Tustin transformation, where $\delta \in \rho(A) \cap \rho(A + LC_m)$.*

Proof: The proof is similar to Theorem 3 and hence can be completed by taking $C_{md} = B_d^*$ and $L_{1d} = K_d^*$. □

3.3. Output feedback regulator design

Considering the unavailability and/or potentially prohibitive costs of installing spatially distributed sensing devices, the implementation of a state feedback compensator is not realistic. Hence, the output feedback regulator is more preferred in practical use. Along this line, the state feedback regulator is extended to an output feedback regulator, which is mathematically described as:

$$u_k = K_d \hat{x}_{k-1} + L_d \hat{q}_k, \ k \geq 1 \tag{30}$$

where $K_d \in \mathcal{L}(X, U)$, $L_d \in \mathcal{L}(\mathbb{C}^n, U)$, where $\hat{x}_{k-1}$ and $\hat{q}_k$ denote the estimated states of the plant and exogenous systems.

Along this line, one can construct Luenberger-type observers for plant and exo-system respectively as follows:

$$\hat{x}_k = A_d \hat{x}_{k-1} + B_d u_k + E_d \hat{d}_k + L_{1d}(y_{mk} - \hat{y}_{mk}) \tag{31a}$$

$$\hat{y}_{mk} = C_{md} \hat{x}_{k-1} + D_{md} u_k + \Upsilon_{md} \hat{d}_k \tag{31b}$$

$$\hat{q}_{k+1} = S_d \hat{q}_k + L_{2d}(y_{rk} - \hat{y}_{rk}) \tag{31c}$$

$$\hat{d}_k = F_d \hat{q}_k \tag{31d}$$

$$\hat{y}_{rk} = Q_d \hat{q}_k \tag{31e}$$

where $\hat{x}_0 \in X$, $\hat{q}_0 = \hat{q}^0 \in \mathbb{C}^n$, $k \geq 1$.

By direct manipulation of Eqs. (30), (31) the following form is obtained:

$$\hat{x}_k^e = \begin{bmatrix} O_1 O_2 \\ 0 \ O_3 \end{bmatrix} \hat{x}_{k-1}^e + \begin{bmatrix} L_{1d} & 0 \\ 0 & L_{2d} \end{bmatrix} \begin{bmatrix} y_{mk} \\ y_{rk} \end{bmatrix} \tag{32a}$$

$$u_k = \begin{bmatrix} K_d \ L_d \end{bmatrix} \hat{x}_{k-1}^e \tag{32b}$$

where $\hat{x}_k^e = [\hat{x}_k; \hat{q}_{k+1}]$, with $k \geq 1$, and

$$O_1 = A_d - L_{1d} C_{md} + (B_d - L_{1d} D_{md}) K_d$$
$$O_2 = (E_d - L_{1d} \Upsilon_{md}) F_d + (B_d - L_{1d} D_{md}) L_d$$
$$O_3 = S_d - L_{2d} Q_d$$

Finally, one can deploy Corollary 1 or Corollary 2 to determine the stabilizing output injection gain L_{1d} of the plant observer and apply pole-placement to find a stabilizing observer gain L_{2d} for the exo-system.

In the ensuing sections, two representative examples (CGLE and KSE) of fluid flow systems are given to illustrate the feasibility and applicability of the proposed regulator design method.

Remark 7. In the output regulation problem, there are two components in the control laws (10) and (30), including a feedback control part accounting for (closed-loop) model stabilization and a feedforward control part ensuring the tracking error converging to zero as time goes to infinity. In general, one can adopt some existing feedback techniques to realize model stabilization of nonlinear distributed parameter systems, e.g., by using interpolants and projections methods [8,40]. However, the feedforward control is much more difficult to find since it is determined by a set of nonlinear partial differential and algebraic equations, which is a nonlinear counterpart of the regulator equations encountered in the linear output regulation problems. The difficulties lie in the solvability of the so-called nonlinear regulator equations. To address that, a zero dynamics design method can be applied as in [11,59], also see [32, Chapter 3] for nonlinear lumped parameter systems. Since this work is focused on the discrete-time linear output regulator design of fluid flow systems, the nonlinear regulator design will not be detailed in this manuscript.

Remark 8. The presented Cayley–Tustin transformation is capable of transforming a continuous-time infinite-dimensional systems with possible unbounded operators (boundary control and observation) into a discrete-time infinite-dimensional model with all bounded operators. However, for the unstable system (e.g. Ginzburg–Landau equation) considered in this work, the corresponding model stabilization via boundary control could not be achieved by using traditional methods, and the most common practice to solve boundary control problem is to use backstepping methods, which is beyond the manuscript scope. Another possible approach is to utilize model predictive controller design proposed in [20]. Since this work is focused on the discrete-time linear output regulator design of fluid flow systems with bounded control and observation operators, the boundary control and observation will not be addressed in this manuscript.

4. Complex Ginzburg Landau flow model

In this section, a linearized complex Ginzburg–Landau equation, which takes form of a complex parabolic partial differential equation, is considered. More specifically, a discrete-time CGLE model is generated without spatial approximation or model reduction using the Cayley–Tustin discretization method. Additionally, a resolvent operator is found in a closed analytic form and deployed in the realization of the discrete CGLE model.

4.1. Model description

Based on the model developments from [2,35], a linearized complex Ginzburg–Landau equation is given as follows:

$$\frac{\partial x}{\partial t}(\bar{\xi}, t) = a_1 \frac{\partial^2 x(\bar{\xi}, t)}{\partial \bar{\xi}^2} + a_2(\bar{\xi}) \frac{\partial x(\bar{\xi}, t)}{\partial \bar{\xi}} + a_3(\bar{\xi}) x(\bar{\xi}, t) \tag{33a}$$

$$x_{\bar{\xi}}(0,t) = \bar{u}(t) \tag{33b}$$

$$x_{\bar{\xi}}(\bar{\xi}_d,t) = 0 \tag{33c}$$

where $x(\bar{\xi},t) \in \bar{\mathcal{X}}$ is a complex-valued function with spatial variable $\bar{\xi} \in [0,\bar{\xi}_d] \subset \mathbb{R}$, and temporal variable $t \in [0,\infty)$. $\bar{\mathcal{X}} = L^2((0,\bar{\xi}_d),\mathbb{C})$ denotes a complex Hilbert space. In addition, a_1 is a positive constant, and $a_2(\bar{\xi})$ and $a_3(\bar{\xi})$ are two complex spatial functions. By applying an invertible state transformation $w(\bar{\xi},t) = x(\bar{\xi},t)g(\bar{\xi})$, $g(\bar{\xi}) = \exp(\frac{1}{2a_1}\int_0^{\bar{\xi}} a_2(\eta)d\eta)$ and spatial scaling $\xi = \frac{\bar{\xi}_d - \bar{\xi}}{\bar{\xi}_d}$, the convective term is eliminated as:

$$\frac{\partial w}{\partial t}(\xi,t) = b_1\frac{\partial^2 w(\xi,t)}{\partial \xi^2} + b_2(\xi)w(\xi,t) \tag{34a}$$

$$w_\xi(1,t) = u(t) \tag{34b}$$

$$w_\xi(0,t) = 0 \tag{34c}$$

with notations:

$$b_1 = \frac{a_1}{\bar{\xi}_d^2} \tag{35a}$$

$$b_2(\xi) = -\frac{1}{2}a_2'(\xi) - \frac{1}{4a_1}a_2^2(\xi) + a_3(\xi) \tag{35b}$$

where $w(\xi,t) \in \mathcal{X} = L^2((0,1),\mathbb{C})$, $\xi \in [0,1]$, and $a_2'(\xi)$ denotes the spatial derivative of $a_2(\xi)$. Moreover, $u(t)$ is the corresponding input of the scaled system (34).

By [55, Rem. 10.1.6], the boundary actuation can be transformed into an abstract in-domain control described by a spatial distribution function $\mathcal{B}(\xi)$ by solving an inner product formula as below:

$$\langle \mathcal{L}_o\phi, \psi\rangle = \langle \phi, \mathcal{A}^*\psi\rangle + \langle G\phi, \mathcal{B}^*\psi\rangle \tag{36}$$

where $\forall\phi \in \mathcal{D}(\mathcal{L}_o)$, $\forall\psi \in \mathcal{D}(\mathcal{A}^*)$, and $\mathcal{L}_o := b_1\frac{\partial^2}{\partial\xi^2} + b_2(\xi)$ with $\mathcal{D}(\mathcal{L}_o) = \mathcal{H}^1((0,1),\mathbb{C})$. The boundary control is denoted by G, namely, $G\phi := \phi_\xi(1)$. By introducing $\mathcal{X}_1 = \mathrm{Ker}\,(G)$, we obtain $\mathcal{A} = \mathcal{L}_o|_{\mathcal{X}_1}$ with the same definition as $\mathcal{L}_o$, but a different domain as $\mathcal{D}(\mathcal{A}) = \{\phi \in \mathcal{X} | \phi \in \mathcal{H}^1((0,1),\mathbb{C}) \cap \mathrm{Ker}\,(G)\}$. It can be found that $\mathcal{A}^* = b_1\frac{\partial^2}{\partial\xi^2} + \overline{b_2(\xi)}$ and $\mathcal{D}(\mathcal{A}^*) = \mathcal{D}(\mathcal{A})$. It is straightforward to obtain

$$\langle G\phi, \mathcal{B}^*\psi\rangle = \phi_\xi(1)\psi^*(1) \tag{37}$$

where $\forall\phi \in \mathcal{D}(\mathcal{L}_o)$, and $\forall\psi \in \mathcal{D}(\mathcal{A}^*)$. Comparing this with the fact that $G\phi = \phi_\xi(l)$, it follows that $\mathcal{B}(\xi) = \delta(\xi - 1)$. For the sake of simplicity, we deploy the approximation $\mathcal{B}(\xi) \approx \frac{1}{2\varepsilon}\mathbf{1}_{[\xi_b-\varepsilon,\xi_b+\varepsilon]}(\xi)$ in what follows, where $\mathbf{1}_{[a,b]}(\xi)$ denotes the spatial shaping function: $\mathbf{1}_{[a,b]}(\xi) = \begin{cases} 1, \xi \in [a,b] \\ 0, \text{otherwise} \end{cases}$.

Therefore, a standard infinite-dimensional state-space model is formulated for the considered CGLE model as:

$$\frac{\partial w}{\partial t}(\xi,t) = \mathcal{A}w(\xi,t) + \mathcal{B}u(t) + \mathcal{E}d(t) \tag{38a}$$

$$y_c(t) = \mathcal{C}_c w(\xi,t) \tag{38b}$$

$$y_m(t) = \mathcal{C}_m w(\xi,t) \tag{38c}$$

where $u(t) \in L^2_{loc}([0,\infty),U)$, $d(t) \in L^2_{loc}([0,\infty),U_d)$, and $y(t) \in L^2_{loc}([0,\infty),Y)$, with U, U_d and Y being finite-dimensional spaces. More specifically, we consider $\dim U = \dim U_d = \dim Y = 1$. In addition, we consider $\mathcal{A} : \mathcal{D}(\mathcal{A}) \subset \mathcal{X} \mapsto \mathcal{X}$ being an infinitesimal generator of a C_0-semigroup $\mathbb{T}(t)$ on $\mathcal{X}$, a bounded control operator $\mathcal{B} \in \mathcal{L}(U,\mathcal{X})$, a point observation operator $\mathcal{C}_c \in \mathcal{L}(\mathcal{X}_1,Y)$, and a bounded disturbance operator $\mathcal{E} \in \mathcal{L}(U_d,\mathcal{X})$. More specifically, we aim to steer a flow at point ξ_c, so the output of interest is given as: $\mathcal{C}_c := \int_0^1 \delta(\xi - \xi_c)(\cdot)d\xi$, where $\delta(\xi - \xi_c)$ denotes the Dirac delta function. For model well-posedness, we employ $\mathcal{C}_\Lambda x = \lim_{\lambda\to+\infty} \mathcal{C}_c\lambda(\lambda I - \mathcal{A})^{-1}x$ to replace $\mathcal{C}_c$, where I is an identity operator, $x \in \mathcal{X}$, $\lambda \in \rho(\mathcal{A})$ (see details in [56]). As for observation, we introduce a bounded operator $\mathcal{C}_m$ as: $\mathcal{C}_m := \int_0^1 \frac{1}{2\upsilon}\mathbf{1}_{[\xi_m-\upsilon,\xi_m+\upsilon]}(\xi)(\cdot)d\xi$. The design objective is to realize output reference tracking, disturbance rejection, and model stabilization. In order to find the stabilizing controller and observer gains, we provide a spectrum analysis that will be utilized in pole-shifting design.

4.2. Spectrum analysis

It can be shown in several ways that for a constant spatial function $b_2(\xi)$ the spectrum of $\mathcal{A}$ can be found analytically as follows:

$$\lambda_n = b_2 - b_1 n^2\pi^2 \tag{39a}$$

$$\phi_n = \sqrt{2}\cos(n\pi\xi) \tag{39b}$$

with $n \in \mathbb{N}$. As for $n = 0$, one has $(\lambda_0,\phi_0) = (\bar{b}_2, \mathbf{1}(\xi))$. However, for an arbitrary complex spatial function $b_2(\xi)$, it is not simple to find the spectrum characteristic of $\mathcal{A}$. For simplicity, we take maximum value (w.r.t. real part) of the spatial function $b_2(\xi)$ as $\bar{b}_2$ to approximate the original function $b_2(\xi)$, resulting in $\mathcal{A} := b_1\frac{\partial^2}{\partial\xi^2} + \bar{b}_2$. Then, the spectrum of $\mathcal{A}$ naturally follows Eq. (39) with b_2 replaced by $\bar{b}_2$, which is given as follows:

$$\lambda_n = \bar{b}_2 - b_1 n^2\pi^2 \tag{40a}$$

$$\phi_n = \sqrt{2}\cos(n\pi\xi) \tag{40b}$$

with $n = 1, 2, \ldots$. For $n = 0$, one has $(\lambda_0,\phi_0) = (\bar{b}_2, \mathbf{1}(\xi))$, which will be further exploited for the output regulator design in the ensuing sections.

4.3. Resolvent operator

One of the most important steps in discrete regulator design is to find the resolvent operator from the continuous model so as to realize the corresponding discrete-time model. To achieve this, Laplace transformation is usually performed on the continuous-time model (38). Considering that the resolvent operator purely depends on $\mathcal{A}$, one can drop $\mathcal{B}$ and $\mathcal{E}$ and directly apply Laplace transformation leading to:

$$\frac{\partial}{\partial\xi}\begin{bmatrix} w(\xi,s) \\ w_\xi(\xi,s)\end{bmatrix} = \begin{bmatrix} 0 & 1 \\ \frac{s-b_2}{b_1} & 0\end{bmatrix}\begin{bmatrix} w(\xi,s) \\ w_\xi(\xi,s)\end{bmatrix} - \begin{bmatrix} 0 \\ \frac{1}{b_1}\end{bmatrix}w(\xi,0)$$

By defining $w_e(\xi,s) = [w(\xi,s); w_\xi(\xi,s)]$, it is straightforward to obtain the solution of $w_e(\xi,s)$ as follow:

$$w_e(\xi,s) = e^{M\xi}w_e(0,s) + \int_0^\xi e^{M(\xi-\eta)}A_0 w(\eta,0)d\eta \tag{41}$$

where

$$A_0 = \begin{bmatrix} 0 \\ -\frac{1}{b_1}\end{bmatrix},\ M = \begin{bmatrix} 0 & 1 \\ \frac{s-b_2}{b_1} & 0\end{bmatrix}$$

Table 1
Parameters considered for the CGLE model (where $j^2 = -1$) [35].

Parameter	Numerical value
a_1	0.01667
$a_2(\bar{\xi})$	$(0.1697 + 0.04939j)\bar{\xi}^2 - (0.1748 + 0.06535j)\bar{\xi} - 0.09061 + 0.001485j$
$a_3(\bar{\xi})$	$(0.1563 - 0.001352j)\bar{\xi}^4 + (-1590 + 0.6278j)\bar{\xi}^3 + (0.3958 - 1.8577j)\bar{\xi}^2 + (-1.6852 + 1.6759j)\bar{\xi} + 1.2645 - 0.2489j$

After some simple algebraic manipulations, one can obtain $e^{M\xi} = [M_{ij}(\xi, s)]_{2\times 2}$, with $i, j = 1, 2$, as below

$$e^{M\xi} = \begin{bmatrix} \cosh(\sqrt{\frac{s-b_2}{b_1}}\xi) & \sqrt{\frac{b_1}{s-b_2}}\sinh(\sqrt{\frac{s-b_2}{b_1}}\xi) \\ \sqrt{\frac{s-b_2}{b_1}}\sinh(\sqrt{\frac{s-b_2}{b_1}}\xi) & \cosh(\sqrt{\frac{s-b_2}{b_1}}\xi) \end{bmatrix}$$

Substituting boundary conditions $w_\xi(1, s) = 0 = w_\xi(0, s)$ into Eq. (41), one can solve for $w(0, s)$ so that the resolvent operator is determined in the closed analytic form:

$$\begin{aligned} &\mathcal{R}(s, \mathcal{A})(\cdot) \\ &= \frac{M_{11}(\xi, s)}{b_1 M_{21}(l, s)} \int_0^1 M_{22}(1-\eta, s)(\cdot)d\eta - \frac{1}{b_1}\int_0^\xi M_{12}(\xi-\eta, s)(\cdot)d\eta \\ &= \frac{1}{\sqrt{b_1(s-b_2)}} \times \Big[-\int_0^\xi \sinh(w_s(\xi-\eta))(\cdot)d\eta \\ &\quad + \frac{\cosh(w_s\xi)}{\sinh(w_s)}\int_0^1 \cosh(w_s(1-\eta))(\cdot)d\eta \Big] \end{aligned} \tag{42}$$

where $w_s = \sqrt{\frac{s-b_2}{b_1}}$. Then, a direct calculation leads to the expressions of $(\mathcal{A}_d, \mathcal{B}_d, \mathcal{C}_d, \mathcal{D}_d)$ as:

$$\begin{aligned} \mathcal{A}_d(\cdot) &= -(\cdot) - \frac{2\delta}{\sqrt{b_1(\delta - b_2)}}\int_0^\xi \sinh(w_\delta(\xi-\eta))(\cdot)d\eta \\ &\quad + \frac{2\delta\cosh(w_\delta\xi)}{\sqrt{b_1(\delta-b_2)}\sinh(w_\delta)}\int_0^1 \cosh(w_\delta(1-\eta))(\cdot)d\eta \end{aligned} \tag{43a}$$

$$\mathcal{B}_d = \begin{cases} \frac{\sqrt{2\delta}}{2\varepsilon(\delta-b_2)}\Big[1 - \cosh(w_\delta(\xi-\xi_b+\varepsilon)) + \\ \qquad \frac{\cosh(w_\delta\xi)\cosh(w_\delta(\xi-\xi_b+\varepsilon))}{\sinh(w_\delta)}\Big], \xi \in [\xi_b-\varepsilon, \xi_b+\varepsilon] \\ \frac{\sqrt{2\delta}\cosh(w_\delta\xi)\cosh(w_\delta(\xi-\xi_b+\varepsilon))}{2\varepsilon(\delta-b_2)\sinh(w_\delta)}, \text{otherwise} \end{cases} \tag{43b}$$

$$\begin{aligned} \mathcal{C}_{cd}(\cdot) &= -\frac{\sqrt{2\delta}}{\sqrt{b_1(\delta-b_2)}}\int_0^{\xi_c} \sinh(w_\delta(\xi_c-\eta))(\cdot)d\eta \\ &\quad + \frac{\sqrt{2\delta}\cosh(w_\delta\xi_c)}{\sqrt{b_1(\delta-b_2)}\sinh(w_\delta)}\int_0^1 \cosh(w_\delta(1-\eta))(\cdot)d\eta \end{aligned} \tag{43c}$$

$$\mathcal{D}_{cd} = \frac{\cosh(w_\delta\xi_c)\cosh(w_\delta(\xi_c-\xi_b+\varepsilon))}{2\varepsilon(\delta-b_2)\sinh(w_\delta)}, \ \xi_c < \xi_b - \varepsilon \tag{43d}$$

where $w_\delta = \sqrt{\frac{\delta-b_2}{b_1}}$. With $\xi_c < \xi_b - \varepsilon < 1$, we note that

$$\lim_{s\to+\infty}\mathcal{G}_c(s) = \lim_{\delta\to+\infty}\mathcal{D}_{cd}(\delta) = 0$$

In a similar fashion, we can obtain analytic expressions of $\mathcal{D}_{md}$ and other discrete operators. With $\xi_m + \upsilon < \xi_b - \varepsilon$, one can further infer that

$$\lim_{s\to+\infty}\mathcal{T}_c(s) = \lim_{\delta\to+\infty}\mathcal{D}_{md}(\delta) = 0$$

which implies that the system (38) is a well-posed regular system [57].

4.4. Simulation study

In the simulation section, the designed discrete-time regulator is implemented to regulate the real part of the controlled output of the linearized CGLE model (38). More specifically, sinusoidal signals generated by the discrete-time exo-system are deployed as disturbance and reference signals. In addition, the model parameters of the considered CGLE model in this work are adopted from [35,46], and are given in Table 1.

In this case, the disturbance distribution is described by $\mathcal{E}(\xi) = \mathbf{1}_{[0,0.5]}(\xi)$, and other numerical parameters are taken as $\Delta\xi = 0.00125$, $h = 0.5$, $\xi_d = 1.5$, $\xi_c = 0.5$, $\xi_b = 0.9$, $\varepsilon = 0.1$, $\xi_m = 0.1$ and $\upsilon = 0.1$. Additionally, the initial condition utilized here is given as: $\hat{w}_0 = (\sqrt{2} - \sqrt{2}i) \times (0.01 \times \cos(2\pi\xi) - 0.0003 \times \cos(4\pi\xi))$. By applying Theorem 2 and Corollary 1, K_d and L_{1d} can be consequently determined. By performing pole placement, the real part of the eigenvalues of $(S_d - L_{2d}Q_d)$ are placed at -0.1. In order to generate sinusoidal signals, we take $S_d = [0.9824, 0.1868; -0.1868, 0.9824]$, $\hat{q}^0 = [-0.4; 1.4]$, $F_d = [0, 0.010]$, and $Q_d = [0.030, 0]$, leading to periodic reference and disturbance signals as: $y_{rk} = 0.03 \times \sin(0.06k\pi)$ and $d_k = 0.01 \times \cos(0.06k\pi)$. Revisiting Eqs. (21b) and (6), the discrete feedforward gain can be solved as $\Gamma_d = [0.0224, 0.0340]$, which completes the control action u_k.

After simulation of 30 seconds, the closed-loop state and output evolution profiles are depicted in Figs. 3 and 4. It is apparent that the designed output regulator can stabilize the originally unstable system, and the spatiotemporal profile shows the expected periodic behaviour. From the perspective of output tracking performance, one can clearly see that the real part of the controlled output follows the desired reference signal and the tracking error converges to zero quickly, which demonstrates the effectiveness of the proposed output regulator design.

5. Kuramoto–Sivashinsky Equation

In this section, a continuous-time nonlinear Kuramoto–Sivashinsky equation (KSE) is introduced to describe the falling thin film dynamics. For the sake of simplicity, a linear KSE is achieved by performing linearization. In the same manner, the Cayley–Tustin transformation is utilized for time discretization for the linear KSE model. Moreover, an explicit closed-form solution is obtained for the corresponding resolvent operator, which is exploited for the discrete-time regulator design.

5.1. KSE model description

In this section, a general nonlinear Kuramoto–Sivashinsky equation with an in-domain actuation is considered as follows [13]:

$$\begin{aligned} &\frac{\partial x}{\partial t}(\zeta, t) + \nu x_{\zeta\zeta\zeta\zeta}(\zeta, t) + x_{\zeta\zeta}(\zeta, t) \\ &+ x_\zeta(\zeta, t)x(\zeta, t) + B(\zeta)u(t) + E(\zeta)d(t) = 0 \end{aligned} \tag{44}$$

with boundary conditions and initial condition:

$$x(0, t) = 0, \ x(l, t) = 0, \ x_\zeta(0, t) = 0, \ x_\zeta(l, t) = 0 \tag{45a}$$

$$x(\zeta, 0) = x_0(\zeta) \tag{45b}$$

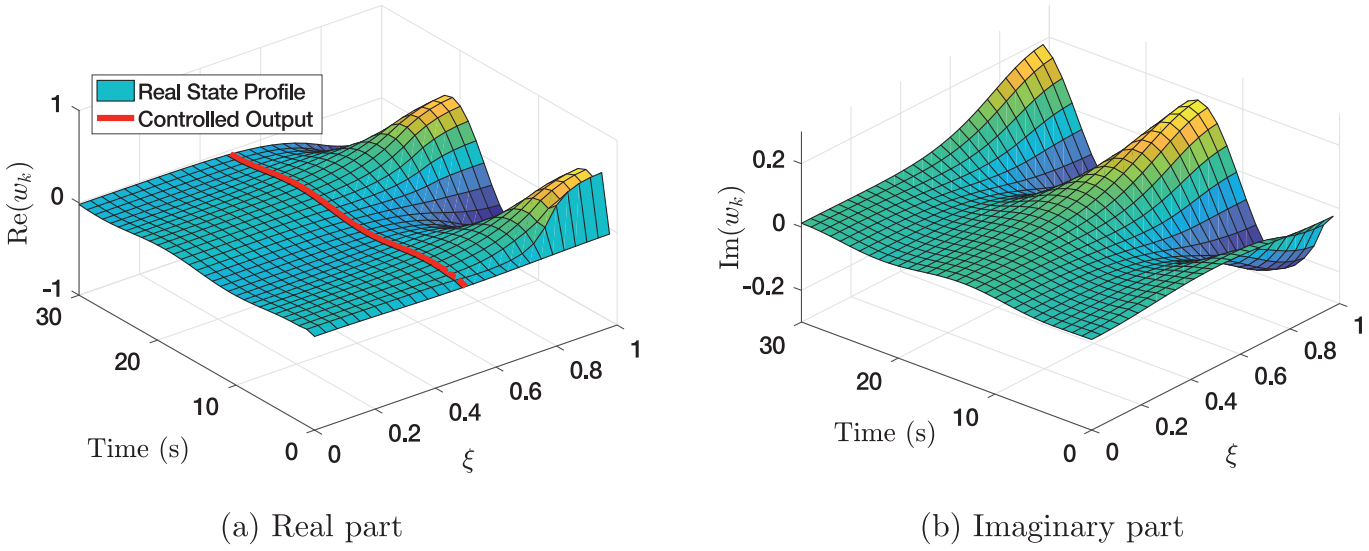

(a) Real part (b) Imaginary part

Fig. 3. State evolution of closed-loop CGLE system in the case of regulation of the real part of the controlled output.

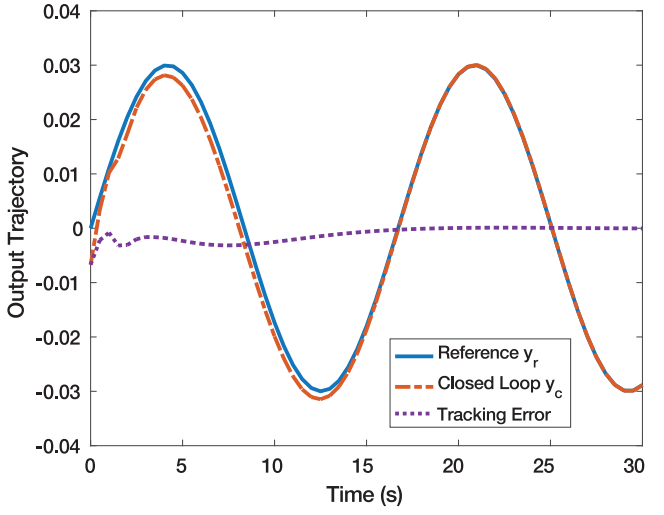

Fig. 4. Output trajectory of closed-loop CGLE system in the case of regulation of the real part of the controlled output.

where x describes the thickness of a thin falling flow, as illustrated in Fig. 2. $t \in [0, \infty)$ and $\zeta \in [0, l]$ denote temporal and spatial variables, respectively. The total length of the vertical pipe is denoted by l. Additionally, x_t represents the first-order temporal derivative of state x, while x_ζ, $x_{\zeta\zeta}$ and $x_{\zeta\zeta\zeta\zeta}$ stand for first-order, second-order and fourth-order derivatives of state x with respect to space. $u(t)$ denotes a manipulated variable representing the angle at which the air front is acting on the film-annulus separation points, and $B(\zeta)$ is a spatial function describing the control action along the vertical pipe. In particular, we consider $B(\zeta) = \frac{1}{2\varepsilon}\mathbf{1}_{[\zeta_b-\varepsilon,\zeta_b+\varepsilon]}(\zeta)$. $d(t)$ represents a distributed disturbance characterized by a bounded spatial function $E(\zeta)$. After linearizing the KSE (44) around the spatially uniform steady state $x_{ss}(\zeta) = 0$, a linear KSE is attained as follow [60]:

$$x_t(\zeta,t) + \nu x_{\zeta\zeta\zeta\zeta}(\zeta,t) + x_{\zeta\zeta}(\zeta,t) + B(\zeta)u(t) + E(\zeta)d(t) = 0 \tag{46}$$

with:

$$x(0,t) = 0,\ x(l,t) = 0,\ x_\zeta(0,t) = 0,\ x_\zeta(l,t) = 0 \tag{47a}$$

$$x(\zeta,0) = x_0(\zeta) \tag{47b}$$

To complete the KSE system, we define a controlled output $y_c(t)$ and a measured output $y_m(t)$ as below:

$$y_c(t) = \mathcal{C}_c x(\zeta,t) \tag{48a}$$

$$y_m(t) = \mathcal{C}_m x(\zeta,t) \tag{48b}$$

where $\mathcal{C}_c$ represents a point observation described by $\mathcal{C}_c(\cdot) = \int_0^l \delta(\zeta-\zeta_c)(\cdot)d\zeta$, with $\delta(\zeta-\zeta_c)$ denoting the Dirac delta function. In other words, the controlled output extracts state information at a specific spatial point ζ_c of interest, i.e., $y_c(t) = x(\zeta_c,t)$. In addition, a bounded operator $\mathcal{C}_m$ is introduced to describe $y_m(t)$ as: $\mathcal{C}_m(\cdot) = \int_0^l \frac{1}{2\upsilon}\mathbf{1}_{[\zeta_m-\upsilon,\zeta_m+\upsilon]}(\zeta)(\cdot)d\zeta$. In doing so, a continuous-time KSE system is constructed in the following abstract state-space form:

$$\frac{\partial x}{\partial t}(\zeta,t) = \mathcal{A}x(\zeta,t) + \mathcal{B}u(t) + \mathcal{E}d(t) \tag{49a}$$

$$y_c(t) = \mathcal{C}_c x(\zeta,t) \tag{49b}$$

$$y_m(t) = \mathcal{C}_m x(\zeta,t) \tag{49c}$$

where $\mathcal{A} := -\nu\frac{\partial^4}{\partial\zeta^4} - \frac{\partial^2}{\partial\zeta^2}$ with domain $\mathcal{D}(\mathcal{A}) = \{\phi(\zeta) \in L_2(0,l) | \phi, \phi_\zeta, \phi_{\zeta\zeta}, \phi_{\zeta\zeta\zeta}$ are abs. con., $\phi_{\zeta\zeta\zeta\zeta} \in L_2(0,l),\ \phi(0) = 0,\ \phi(l) = 0,\ \phi_\zeta(0) = 0, \phi_\zeta(l) = 0\}$. In addition, we have $\mathcal{B} := B(\zeta)$ and $\mathcal{E} := E(\zeta)$. This standard model structure taking the same form as Eq. (1) is suitable for model time discretization through the Cayley–Tustin approach as described previously.

5.2. KSE resolvent

In a similar manner as we solved the resolvent operator of CGLE model, we aim to determine the resolvent operator of KSE model in this section. Differently, it needs more complex manipulation to solve for the KSE resolvent operator $\mathcal{R}$ owing to the higher order derivatives in the state evolution operator $\mathcal{A} := -\nu\frac{\partial^4}{\partial\zeta^4} - \frac{\partial^2}{\partial\zeta^2}$. By directly applying Laplace transform to the linearized Kuramoto–Sivashinsky Eq. (46) and ignoring the input and disturbance, one achieves the following:

$$x_{\zeta\zeta\zeta\zeta}(\zeta,s) = -\frac{s}{\nu}x(\zeta,s) - \frac{1}{\nu}x_{\zeta\zeta}(\zeta,s) + \frac{1}{\nu}x_0(\zeta) \tag{50}$$

To utilize boundary conditions for solving the state solution, we introduce new state derivatives to Eq. (50) as follows:

$$\frac{\partial \mathbf{x}}{\partial \zeta} = A\mathbf{x} + \mathbf{x}_0 \tag{51}$$

where $\mathbf{x} = [x; x_\zeta; x_{\zeta\zeta}; x_{\zeta\zeta\zeta}]$, $\mathbf{x}_0 = [0; 0; 0; \frac{1}{\nu}x_0(\zeta)]$, and

$$A = \begin{bmatrix} 0 & 1 & 0 & 0 \\ 0 & 0 & 1 & 0 \\ 0 & 0 & 0 & 1 \\ -\frac{s}{\nu} & 0 & -\frac{1}{\nu} & 0 \end{bmatrix}$$

Direct integration of Eq. (51) leads to:

$$\mathbf{x}(\zeta, s) = e^{A\zeta}\mathbf{x}(0, s) + \int_0^\zeta e^{A(\zeta-\eta)}\mathbf{x}_0(\eta)d\eta \tag{52}$$

where $e^{A\zeta} = [a_{ij}(\zeta, s)]_{4\times 4}$, with $i, j = 1, 2, 3, 4$. Thus, substituting the boundary conditions $x(0, s) = 0$ and $x_\zeta(0, s) = 0$ into Eq. (52) leads to the following simplification:

$$\begin{bmatrix} x(\zeta, s) \\ x_\zeta(\zeta, s) \end{bmatrix} = \begin{bmatrix} a_{13}(\zeta, s) a_{14}(\zeta, s) \\ a_{23}(\zeta, s) a_{24}(\zeta, s) \end{bmatrix} \begin{bmatrix} x_{\zeta\zeta}(0, s) \\ x_{\zeta\zeta\zeta}(0, s) \end{bmatrix} + \int_0^\zeta \begin{bmatrix} a_{14}(\zeta - \eta, s) \\ a_{24}(\zeta - \eta, s) \end{bmatrix} x_0(\eta)d\eta \tag{53}$$

Then, the remaining two boundary conditions $x(l, s) = 0$ and $x_\zeta(l, s) = 0$ in Eq. (47a) are deployed in Eq. (53) such that $x_{\zeta\zeta}(0, s)$ and $x_{\zeta\zeta\zeta}(0, s)$ can be determined as follows:

$$\begin{bmatrix} x_{\zeta\zeta}(0, s) \\ x_{\zeta\zeta\zeta}(0, s) \end{bmatrix} = -\frac{1}{\nu} M^{-1} \int_0^l \begin{bmatrix} a_{14}(l - \eta, s) \\ a_{24}(l - \eta, s) \end{bmatrix} x_0(\eta)d\eta \tag{54}$$

where $M = [a_{13}(l, s), a_{14}(l, s); a_{23}(l, s), a_{24}(l, s)]$. The invertibility of M must be checked to ensure that Eq. (54) holds.

Finally, one can obtain the solution of $x(\zeta, s)$ by plugging Eq. (54) into Eq. (53), which leads to the associated resolvent operator of the KSE system as follows:

$$\begin{aligned} &\mathcal{R}(\zeta, \mathcal{A})(\cdot) \\ &= \frac{1}{\nu}\int_0^\zeta a_{14}(\zeta - \eta, s)(\cdot)d\eta \\ &+ \frac{a_{13}(\zeta, s)}{\nu[a_{23}(l, s)a_{14}(l, s) - a_{13}(l, s)a_{24}(l, s)]} \\ &\times \int_0^l [a_{14}(l - \eta, s)a_{24}(l, s) - a_{24}(l - \eta, s)a_{14}(l, s)](\cdot)d\eta \\ &- \frac{a_{14}(\zeta, s)}{\nu[a_{23}(l, s)a_{14}(l, s) - a_{13}(l, s)a_{24}(l, s)]} \\ &\times \int_0^l [a_{14}(l - \eta, s)a_{23}(l, s) - a_{24}(l - \eta, s)a_{13}(l, s)](\cdot)d\eta \end{aligned} \tag{55}$$

where due to the specific structure of A, an analytic expression for the resolvent operator is found by:

$$a_{23}(\zeta, s) = \frac{\nu(\varpi \sinh(\varpi\zeta) - \omega \sinh(\omega\zeta))}{\sqrt{1 - 4s\nu}} \tag{56a}$$

$$a_{13}(\zeta, s) = \frac{\nu(\cosh(\varpi\zeta) - \cosh(\omega\zeta))}{\sqrt{1 - 4s\nu}} \tag{56b}$$

$$a_{24}(\zeta, s) = \frac{\nu(\cosh(\varpi\zeta) - \cosh(\omega\zeta))}{\sqrt{1 - 4s\nu}} \tag{56c}$$

$$\begin{aligned} a_{14}(\zeta, s) = &\frac{\left(1 - \sqrt{1 - 4s\nu}\right)}{4s^2\sqrt{(2 - 8s\nu)}} \times \left[\left(2s\nu - 1 - \sqrt{1 - 4s\nu}\right)\right. \\ &\left. \times \sqrt{2}\varpi \sinh(\varpi\zeta) + 2s\nu\sqrt{2}\omega \sinh(\omega\zeta)\right] \end{aligned} \tag{56d}$$

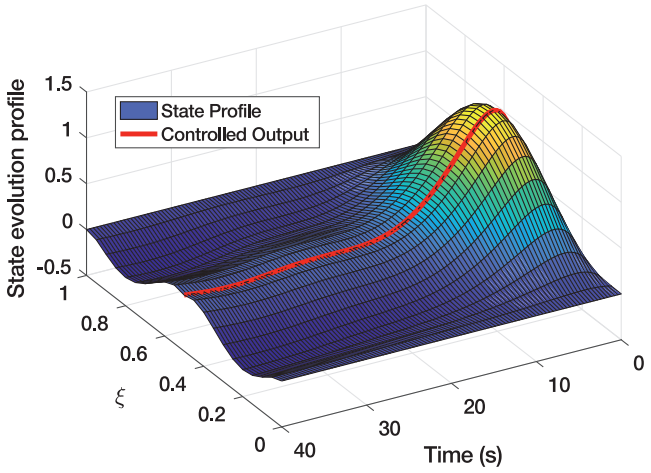

Fig. 5. State evolution of the closed-loop KSE system.

where $\varpi = \sqrt{\frac{-1+\sqrt{1-4s\nu}}{2\nu}}$ and $\omega = \sqrt{\frac{-1-\sqrt{1-4s\nu}}{2\nu}}$. It is observed that, for a given positive real s, ϖ stays as a complex number while ω can be a complex or real number with different choices of ν. Due to the existence and multiplication with hyperbolic functions ("sinh" and "cosh"), it is straightforward to check that $a_{ij}(\zeta, s) \in L^2((0, l), \mathbb{R})$, $\forall s \in \mathbb{R}$, with $i, j = 1, 2, 3, 4$.

The closed-form expressions of discrete-time operators in Eq. (4) corresponding to the discrete KSE system can be determined by simply substituting Eqs. (55), (56) back into Eq. (5). By comparing the order of s in $\mathcal{R}(\zeta, \mathcal{A})$, it can be shown that for given $\xi_c = 0.5$ and $\xi_m + \upsilon \le \xi_b - \varepsilon$

$$\lim_{s\to+\infty} \mathcal{G}_c(s) = \lim_{\delta\to+\infty} \mathcal{D}_{cd}(\delta) = 0$$

$$\lim_{s\to+\infty} \mathcal{T}_c(s) = \lim_{\delta\to+\infty} \mathcal{D}_{md}(\delta) = 0$$

which implies that the system (49) is a well-posed regular system [57].

5.3. Simulation study

In this section, the proposed discrete-time output regulator is implemented to the KSE system and the results are discussed. To demonstrate the effectiveness of the developed regulator, we consider an unstable KSE with $\nu = -3$. The characteristic equation is found by $\nu s^4 + s^2 = \lambda$ (or equivalently written as $\left(s^2 + \frac{1}{2\nu}\right)^2 - \frac{\lambda}{\nu} - \frac{1}{4\nu^2} = 0$), so the eigenvalue spectrum is roughly given by the range $(-\infty, \frac{1}{4\nu}]$ [60]. By revisiting Theorem 2 and Corollary 1, K_d and L_{1d} can be found.

To achieve asymptotic tracking and disturbance rejection of periodic signals, we take $S_d = [0.9995, 0.0314; -0.0314, 0.9995]$, $\hat{q}^0 = [-0.2; 1.2]$, $F_d = [0, 0.1]$, $Q_d = [0.01, 0]$, $\mathcal{E}(\zeta) = \mathbf{1}_{[0,1]}(\zeta)$, $\zeta_b = 0.98$, $\varepsilon = 0.01$, $\zeta_m = 0.1$, $\upsilon = 0.1$, and $\zeta_c = 0.5$. The reference and disturbance signals are generated as: $d_k = 0.1 \times \cos(0.009k\pi)$ and $y_{rk} = 0.01 \times \sin(0.009k\pi)$. Using Eq. (21b) and Eq. (6), the discrete feedforward gain is found as $\Gamma_d = [2640.6559, -23.2574]$, which leads to the control law u_k. Additionally, pole placement is applied to move the real part of eigenvalues of $(S_d - L_{2d}Q_d)$ to -0.5.

The simulated pipe length is taken as $l = 1$m with a spatial interval $\Delta l = 0.005$m. Moreover, a time discretization interval $h = 0.1$s is chosen with total simulation time of 40 seconds. As shown in Fig. 5, the state is steered to reject a cosine disturbance and follow a sinusoid wave using the closed-loop control. As for the output tracking performance, it is apparent that the controlled output rapidly converges to the desired reference and the tracking error

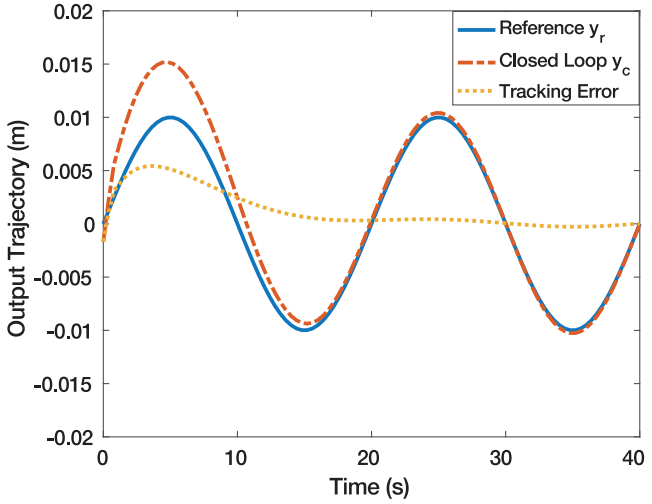

Fig. 6. Output regulation performance of the closed-loop KSE system.

goes to near zero around 30s, as illustrated in Fig. 6, which further verifies the feasibility of the proposed regulator design.

6. Conclusion

In this work, discrete-time output regulators are designed for PDE model-based fluid flow manipulation and regulation. To model the vortex shedding process and falling thin film dynamics, the linearized complex Ginzburg–Landau and Kuramoto–Sivashinsky models are utilized. For realistic implementation of regulators in digital computer systems, the Cayley–Tustin time discretization method is utilized for discrete-in-time analysis with system properties preserved and no spatial approximation. Standard finite-dimensional continuous-time regulator design framework is extended to an infinite-dimensional discrete-time setting with application to CGLE and KSE systems. As key components for the formulation of a discrete-time model (A_d, B_d, C_d, D_d), the resolvent operators corresponding to CGLE and KSE are found in analytic forms, which are used to show the well-posedness of CGLE and KSE models. Simulation results show that the developed design method is capable of stabilizing the system, tracking the periodic output references in the CGLE model and higher-order dynamics in the KSE case. Undesired periodic disturbance signals are rejected for both systems. In the future work, the implementation and realization of the proposed design will be explored experimentally on vortex shedding and falling thin film control problems.

Declaration of Competing Interest

None.

Supplementary material

Supplementary material associated with this article can be found, in the online version, at doi:10.1016/j.ejcon.2020.10.005.

References

[1] O.M. Aamo, M. Krstic, Global stabilization of a nonlinear Ginzburg-Landau model of vortex shedding, European Journal of Control 10 (2) (2004) 105–116.
[2] O.M. Aamo, A. Smyshlyaev, M. Krstic, Boundary control of the linearized Ginzburg–Landau model of vortex shedding, SIAM journal on control and optimization 43 (6) (2005) 1953–1971.
[3] O.M. Aamo, A. Smyshlyaev, M. Krstic, B.A. Foss, Stabilization of a Ginzburg-Landau model of vortex shedding by output feedback boundary control, in: 2004 43rd IEEE Conference on Decision and Control (CDC)(IEEE Cat. No. 04CH37601), 3, IEEE, 2004, pp. 2409–2416.
[4] O.M. Aamo, A. Smyshlyaev, M. Krstic, B.A. Foss, Output feedback boundary control of a Ginzburg–Landau model of vortex shedding, IEEE Transactions on Automatic Control 52 (4) (2007) 742–748.
[5] A. Armaou, P.D. Christofides, Feedback control of the Kuramoto–Sivashinsky equation, Physica D: Nonlinear Phenomena 137 (1-2) (2000) 49–61.
[6] D. Arov, I. Gavrilyuk, V. Makarov, Representation and approximation of solutions of initial value problems for differential equations in Hilbert space based on the Cayley transform, Pitman Research Notes in Mathematics Series (1995). 40–40
[7] D.Z. Arov, I.P. Gavrilyuk, A method for solving initial value problems for linear differential equations in Hilbert space based on the Cayley transform, Numerical functional analysis and optimization 14 (5-6) (1993) 459–473.
[8] A. Azouani, E. Olson, E.S. Titi, Continuous data assimilation using general interpolant observables, Journal of Nonlinear Science 24 (2) (2014) 277–304.
[9] E. Berger, Suppression of vortex shedding and turbulence behind oscillating cylinders, The Physics of Fluids 10 (9) (1967) S191–S193.
[10] C. Byrnes, I.G. Laukó, D.S. Gilliam, V.I. Shubov, Output regulation for linear distributed parameter systems, IEEE Transactions on Automatic Control 45 (12) (2000) 2236–2252.
[11] C.I. Byrnes, D.S. Gilliam, C. Hu, V.I. Shubov, Zero dynamics boundary control for regulation of the Kuramoto–Sivashinsky equation, Mathematical and Computer Modelling 52 (5-6) (2010) 875–891.
[12] C.-J. Chen, H.-C. Chen, Finite analytic numerical method for unsteady two-dimensional Navier-Stokes equations, Journal of Computational Physics 53 (2) (1984) 209–226.
[13] L.-H. Chen, H.-C. Chang, Nonlinear waves on liquid film surfaces-II. Bifurcation analyses of the long-wave equation, Chemical Engineering Science 41 (10) (1986) 2477–2486.
[14] P.D. Christofides, A. Armaou, Global stabilization of the Kuramoto–Sivashinsky equation via distributed output feedback control, Systems & Control Letters 39 (4) (2000) 283–294.
[15] K. Cohen, S. Siegel, T. McLaughlin, E. Gillies, J. Myatt, Closed-loop approaches to control of a wake flow modeled by the Ginzburg–Landau equation, Computers & Fluids 34 (8) (2005) 927–949.
[16] R.F. Curtain, J.C. Oostveen, Bilinear transformations between discrete-and continuous-time infinite-dimensional linear systems, in: Proceedings of the Fourth International Symposium on Methods and Models in Automation and Robots,Poland (1997) 861–870.
[17] R.F. Curtain, H. Zwart, An introduction to Infinite-Dimensional Linear Systems Theory, Springer-Verlag, New York, 1995.
[18] S. Dubljevic, Boundary model predictive control of Kuramoto–Sivashinsky equation with input and state constraints, Computers & Chemical Engineering 34 (10) (2010) 1655–1661.
[19] S. Dubljevic, Model predictive control of Kuramoto–Sivashinsky equation with state and input constraints, Chemical Engineering Science 65 (15) (2010) 4388–4396.
[20] S. Dubljevic, J.-P. Humaloja, Model predictive control for regular linear systems, Automatica 119 (2020) 109066.
[21] B.A. Francis, W.M. Wonham, The internal model principle of control theory, Automatica 12 (5) (1976) 457–465.
[22] I. Gavrilyuk, V. Makarov, Representation and approximation of the solution of an initial value problem for a first order differential equation in banach spaces, Zeitschrift für Analysis und ihre Anwendungen 15 (2) (1996) 495–527.
[23] I. Gavrilyuk, R. Melniky, Constructive approximations of the convection-diffusion-absorption equation based on the Cayley transform technique, in: Computational Mechanics: New Trends and Applications (Proceedings of the Fourth World Congress on Computational Mechanics), CIMNE/IACM, 1998, pp. 1–14.
[24] I.P. Gavrilyuk, V.L. Makarov, The Cayley transform and the solution of an initial value problem for a first order differential equation with an unbounded operator coefficient in Hilbert space, Numerical Functional Analysis and Optimization 15 (5-6) (1994) 583–598.
[25] I.P. Gavrilyuk, V.L. Makarov, Explicit and approximate solutions of second-order evolution differential equations in Hilbert space, Numerical Methods for Partial Differential Equations: An International Journal 15 (1) (1999) 111–131.
[26] I.P. Gavrilyuk, V.L. Makarov, N.V. Mayko, Weighted estimates of the Cayley transform method for abstract differential equations, Computational Methods in Applied Mathematics 1 (ahead-of-print) (2020).
[27] M.D. Gunzburger, H.-C. Lee, Feedback control of Karman vortex shedding, Journal of applied mechanics 63 (3) (1996) 828–835.
[28] P. Guzmán, S. Marx, E. Cerpa, Stabilization of the linear Kuramoto-Sivashinsky equation with a delayed boundary control, in: in Proc. 3rd IFAC CPDE/CDPS Joint Workshop, IFAC, 2019.
[29] E. Hairer, C. Lubich, G. Wanner, Geometric numerical integration: structure-preserving algorithms for ordinary differential equations, 31, Springer Science & Business Media, 2006.
[30] V. Havu, J. Malinen, The Cayley transform as a time discretization scheme, Numerical Functional Analysis and Optimization 28 (7-8) (2007) 825–851.
[31] R.D. Henderson, Details of the drag curve near the onset of vortex shedding, Physics of Fluids 7 (9) (1995) 2102–2104.
[32] J. Huang, Nonlinear output regulation: theory and applications, 8, SIAM, 2004.
[33] X. Huang, Feedback control of vortex shedding from a circular cylinder, Experiments in Fluids 20 (3) (1996) 218–224.
[34] P. Huerre, P.A. Monkewitz, Local and global instabilities in spatially developing flows, Annual review of fluid mechanics 22 (1) (1990) 473–537.
[35] M. Izadi, C.R. Koch, S.S. Dubljevic, Model predictive control of Ginzburg-Lan-

dau equation, in: Active Flow and Combustion Control 2018, Springer, 2019, pp. 75–90.
[36] W. Kang, E. Fridman, Distributed sampled-data control of Kuramoto–Sivashinsky equation, Automatica 95 (2018) 514–524.
[37] M. Krstic, A. Smyshlyaev, Boundary control of PDEs: A course on backstepping designs, 16, Siam, 2008.
[38] Y. Kuramoto, T. Tsuzuki, On the formation of dissipative structures in reaction-diffusion systems: reductive perturbation approach, Progress of Theoretical Physics 54 (3) (1975) 687–699.
[39] W.-J. Liu, M. Krstić, Stability enhancement by boundary control in the Kuramoto–Sivashinsky equation, Nonlinear Analysis: Theory, Methods & Applications 43 (4) (2001) 485–507.
[40] E. Lunasin, E.S. Titi, Finite determining parameters feedback control for distributed nonlinear dissipative systems-a computational study, Evolution Equations & Control Theory 6 (4) (2017) 535–557.
[41] J. Malinen, Tustin's method for final state approximation of conservative dynamical systems, IFAC Proceedings Volumes 44 (1) (2011) 4564–4569.
[42] N. Mayko, Super-exponential rate of convergence of the Cayley transform method for an abstract differential equation, Cybernetics and Systems Analysis (2020) 1–12.
[43] D. Michelson, G. Sivashinsky, Nonlinear analysis of hydrodynamic instability in laminar flames: II. numerical experiments, Acta Astronautica 4 (11-12) (1977) 1207–1221.
[44] M. Milovanovic, O.M. Aamo, Attenuation of vortex shedding in CFD simulations by model-based output feedback control, in: 49th IEEE Conference on Decision and Control (CDC), IEEE, 2010, pp. 2979–2984.
[45] M. Milovanovic, O.M. Aamo, Stabilization of 3D Ginzburg-Landau equation by model-based output feedback control, IFAC Proceedings Volumes 44 (1) (2011) 14435–14439.
[46] M. Milovanovic, O.M. Aamo, Attenuation of vortex shedding by model-based output feedback control, IEEE Transactions on Control Systems Technology 21 (3) (2012) 617–625.
[47] M. Milovanovic, M. Grayer, J. Michielsen, O.M. Aamo, Model-based stabilization of vortex shedding with CFD verification, in: Proceedings of the 48h IEEE Conference on Decision and Control (CDC) held jointly with 2009 28th Chinese Control Conference, IEEE, 2009, pp. 8252–8257.
[48] M.R. Opmeer, R.F. Curtain, New Riccati equations for well-posed linear systems, Systems & control letters 52 (5) (2004) 339–347.
[49] P. Poncet, Topological aspects of three-dimensional wakes behind rotary oscillating cylinders, Journal of Fluid Mechanics 517 (2004) 27–53.
[50] P. Poncet, G.-H. Cottet, P. Koumoutsakos, Control of three-dimensional wakes using evolution strategies, Comptes Rendus Mecanique 333 (1) (2005) 65–77.
[51] K. Roussopoulos, Feedback control of vortex shedding at low Reynolds numbers, Journal of Fluid Mechanics 248 (1993) 267–296.
[52] K. Roussopoulos, P.A. Monkewitz, Nonlinear modelling of vortex shedding control in cylinder wakes, Physica D: Nonlinear Phenomena 97 (1-3) (1996) 264–273.
[53] G. Sivashinsky, Nonlinear analysis of hydrodynamic instability in laminar flames: I. derivation of basic equations, in: Dynamics of Curved Fronts, Elsevier, 1988, pp. 459–488.
[54] O. Staffans, Well-posed linear systems, 103, Cambridge University Press, 2005.
[55] M. Tucsnak, G. Weiss, Observation and control for operator semigroups, Springer Science & Business Media, 2009.
[56] M. Tucsnak, G. Weiss, Well-posed systems–the LTI case and beyond, Automatica 50 (7) (2014) 1757–1779.
[57] G. Weiss, Transfer functions of regular linear systems. I. characterizations of regularity, Transactions of the American Mathematical Society 342 (2) (1994) 827–854.
[58] J.F. Williams, B. Zhao, The active control of vortex shedding, Journal of Fluids and Structures 3 (2) (1989) 115–122.
[59] K. Yang, J. Zheng, G. Zhu, Asymptotic output tracking for a class of semilinear parabolic equations: A semianalytical approach, International Journal of Robust and Nonlinear Control 29 (8) (2019) 2471–2493.
[60] Y. Yang, S. Dubljevic, Boundary model predictive control of thin film thickness modelled by the Kuramoto–Sivashinsky equation with input and state constraints, Journal of Process Control 23 (9) (2013) 1362–1379.